

New magnetic nanostructured materials: focus on biomedical applications

G.V. Kurlyandskaya

University of the Basque Country UPV-EHU, Bilbao, Spain

In collaboration with

Ural Federal University, Ekaterinburg, Russia

Institute of Electrophysics UD RAS, Ekaterinburg, Russia

University of Maryland, College Park, USA

East-Siberian State Academy of Education, Irkutsk, Russia

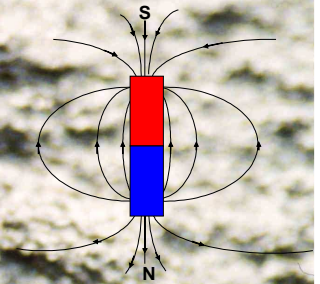
0.1 mm


SUPPLEMENTAL MATERIALS

for the Second Conference on Nanotechnology for Biological
and Biomedical Applications (Nano-Bio-Med 2013)

Introduction to **Bio**magnetic Sensors

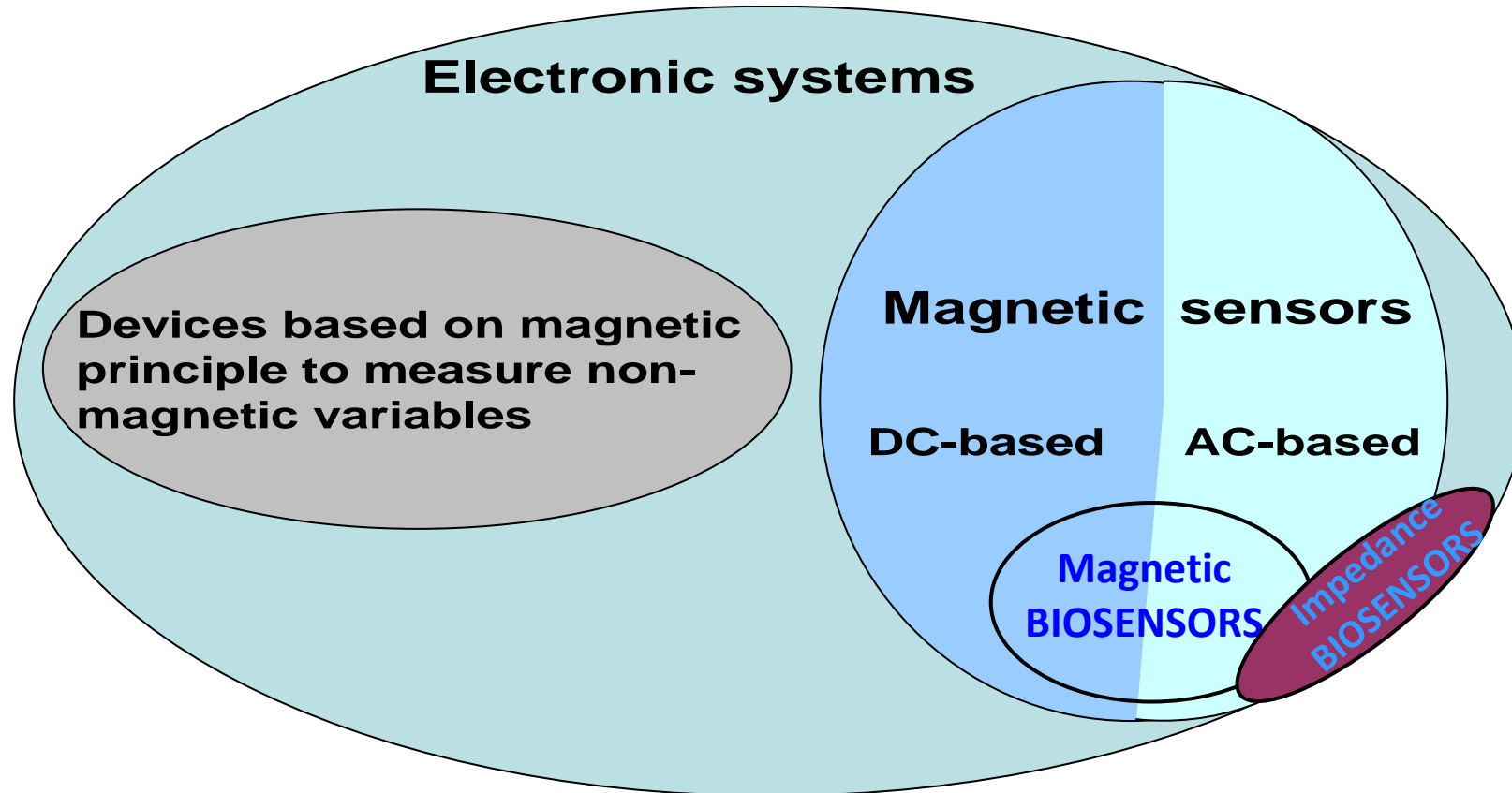
Biosensor and magnetic biosensor definition
Classification of non-magnetic biosensors
Classification of magnetic biosensors
The bead array counter concept
Basic requirements for magnetic labels



Magnetic sensors were introduced long ago to the field of biomedical research focused on the development of advanced diagnostic tools. There are two principal types of biomedical applications: analysis of electric and magnetic properties of living systems closely related to their functionality and analysis of the requested specific properties of the bioanalytes.

SENSOR + BIO + MAGNETIC

Electronic - having components such as microchips and transistors (to control and direct electric currents)



Sensor - sensitive element → transducer → amplifier → filter → analog /digital converter

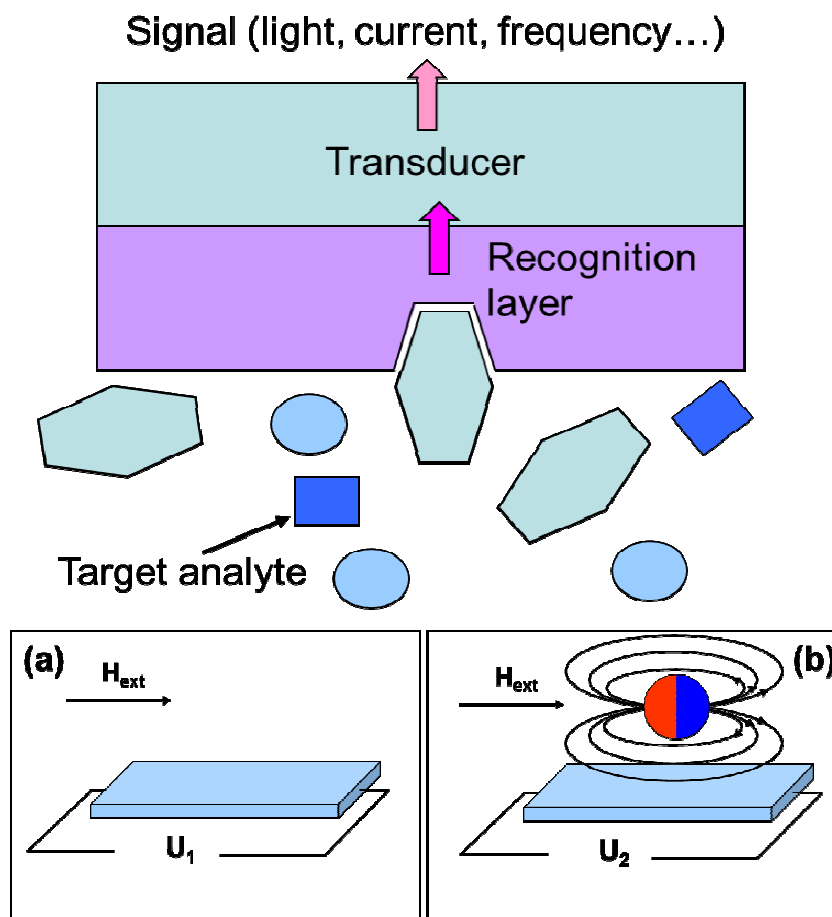
A transducer is a device which converts energy from one form to another.

A biosensor is a compact analytical device incorporating a biological or biologically derived sensitive element, integrated in or associated with a physicochemical transducer [1-2].

In general magnetic biosensors can be classified as detection methods employing markers [2-3] and marker-free detection methods [4-5].

Magnetic biosensor is a compact analytical device incorporating a biological, a biologically derived or a biomimetic material intimately associated with a physicochemical magnetic transducer or transducing microsystem .

A magnetic sensor is a device which measures changes in a magnetic field, i.e. a magnetic transducer converts a magnetic field variation into a change of frequency, current, voltage etc.



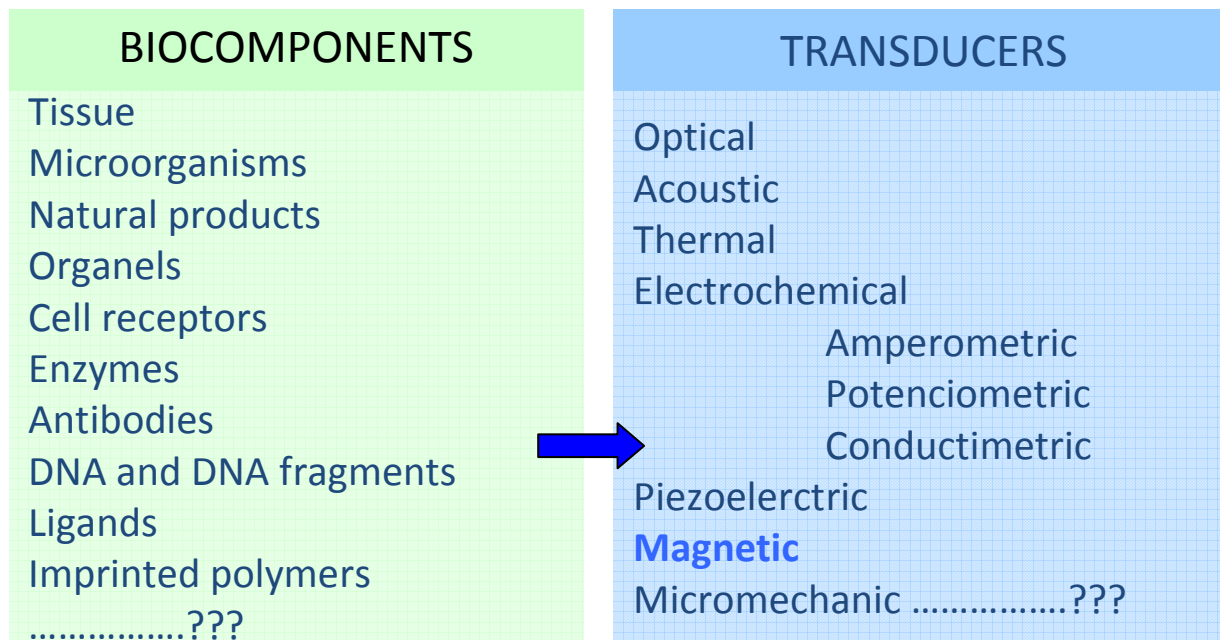
[1] A.P.F. Turner, Biosensors—sense and sensitivity. *Science* **290** (2000) 1315–1317.

[2] D. R. Baselt, G. U. Lee, M. Natesan, S. W. Metzger, P. E. Sheehan and R. A. Colton, A biosensor based on magnetoresistance technology. *Biosensors and Bioelectronics*, **13** (1998) 731-739.

[3] P.-A. Besse, G. Boero, M. Demierre, V. Pott and R. Popovic, Detection of single magnetic microbead using a miniaturized silicon Hall sensor. *Applied Physics Letters*, **80** (2002) 4199–4201.

[4] C. Ruan, K. Zeng, O. K. Varghese and C. A. Grimes, A staphylococcal enterotoxin B magnetoelastic immunosensor. *Biosensors and Bioelectronics*, **20** (2004) 585–591.

[5] G. V. Kurlyandskaya and V. Fal Miyar, Surface modified amorphous ribbon based magnetoimpedance biosensor. *Biosensors and Bioelectronics*, **22** (2007) 2341–2345.



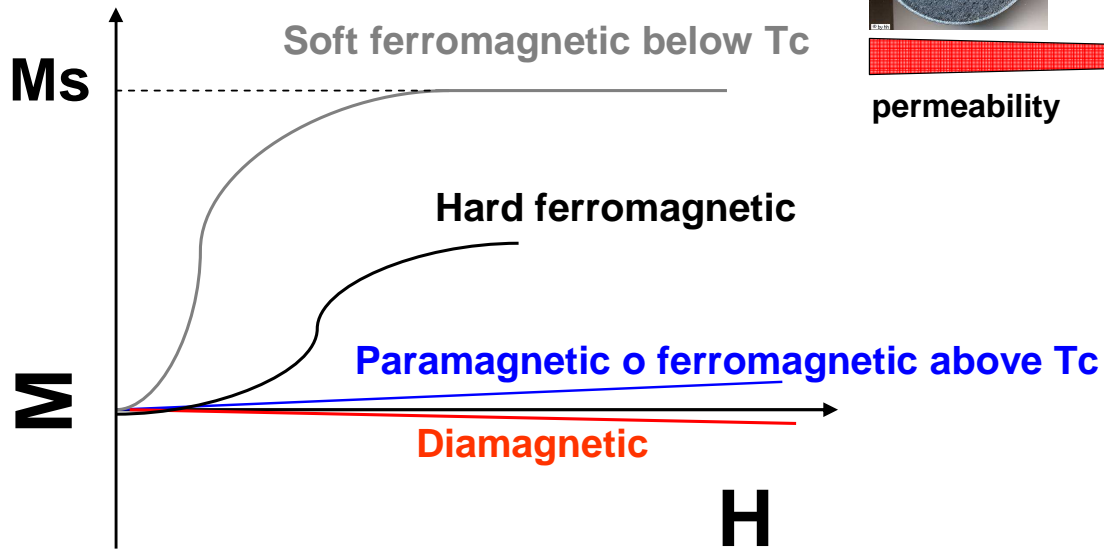
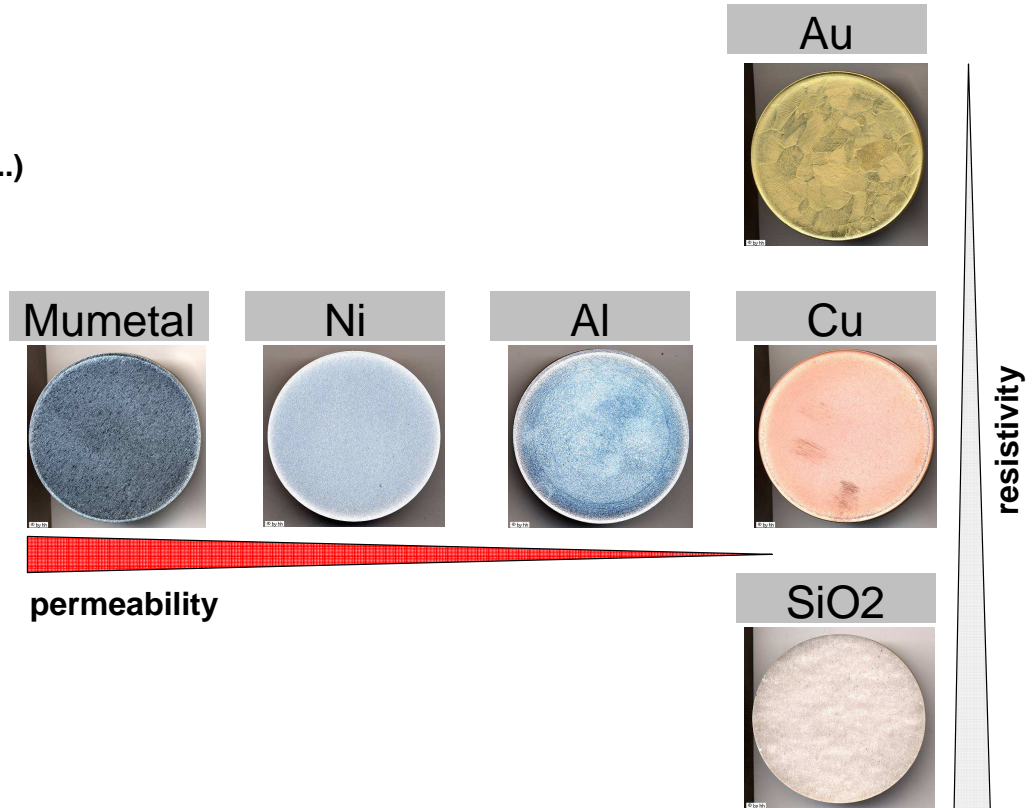
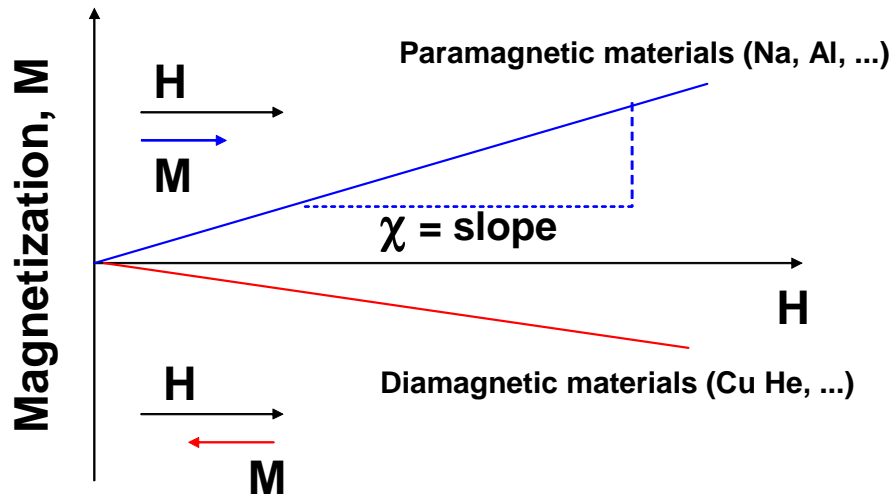
CLASSIFICATION OF NON-MAGNETIC BIOSENSORS

Detection methods employing markers

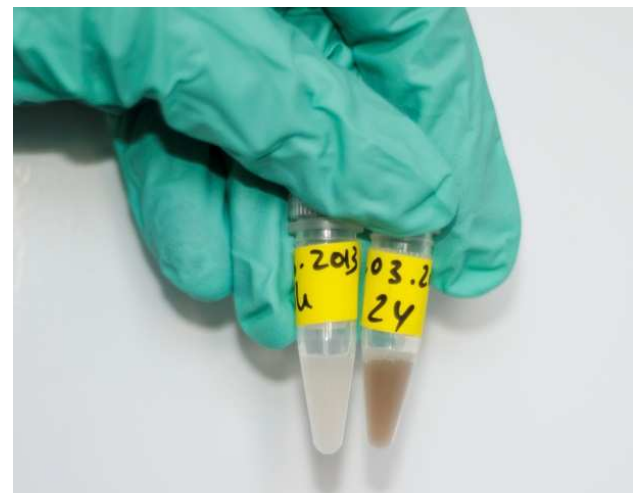
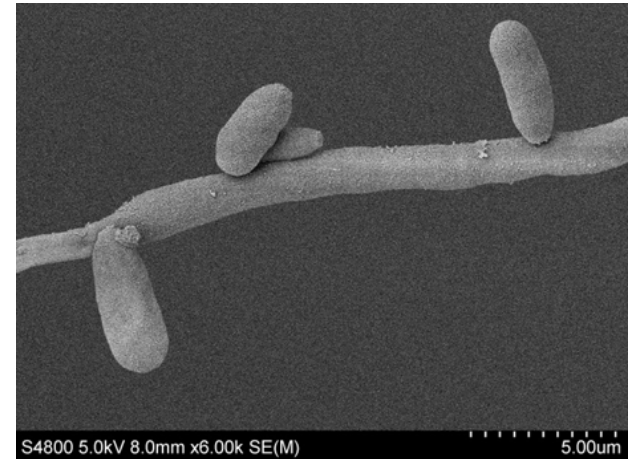
Fluorescent detection
Nanoparticle based detection
Electrochemical detection
Radioactive detection

Label free detection methods

Mass sensitive detection
Charge sensitive detection
Refractive index sensitive detection
Electrochemical oxidation of guanine bases

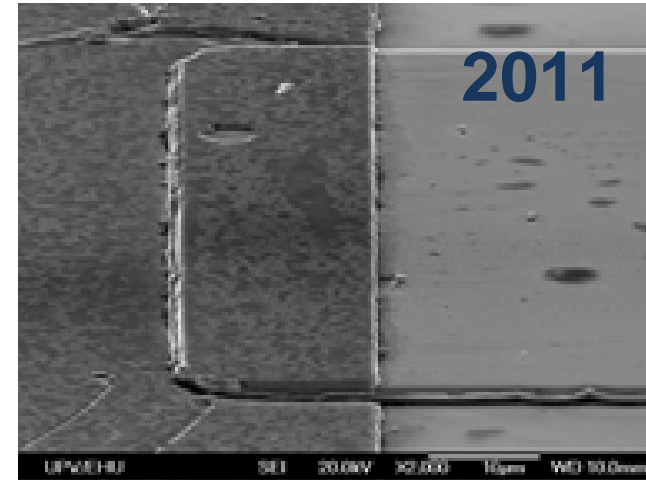
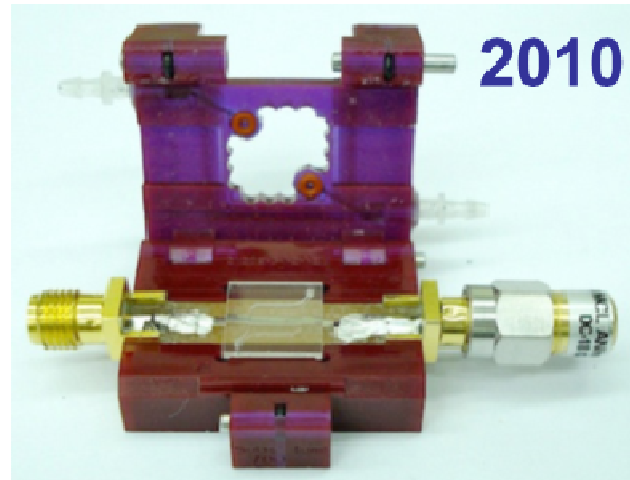
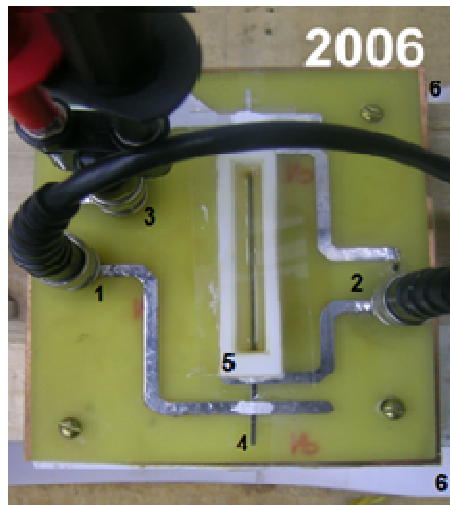


Substance	susceptibility x 10 ⁻⁶
Air	+ 0.34
Water	- 9.05
Arterial blood	- 9.1
Venous blood	- 8.4
Oxygenized erythrocytes	- 9.03
Desoxygenized erythrocytes	+ 3.88
Muscle	- 9.0
Liver	- 8.8
Bone	- 10



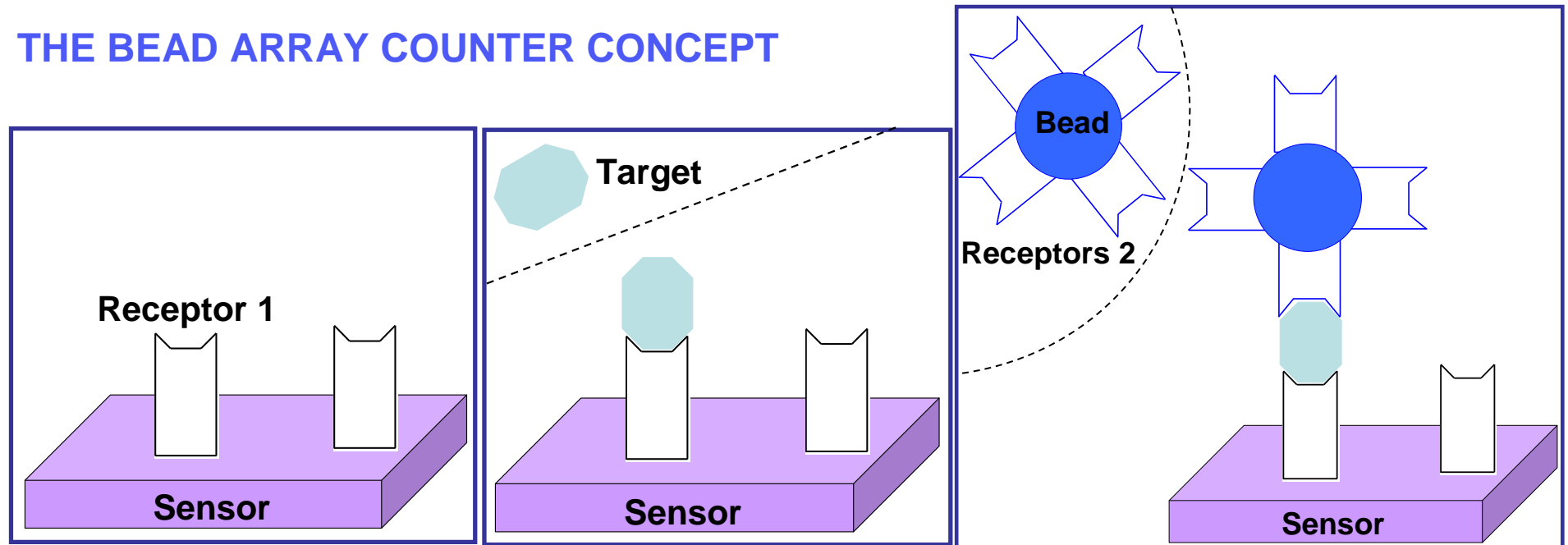
Body liquids and tissues are hardly magnetic by nature, which helps to improve the detection limit of magnetic biosensors and eliminate interference effects.

For a long time the development of magnetic biosensors was suppressed because of their limited sensitivity and/or big size. The description of the first “magnetic biosensor” was reported in 1998 by Baselt et al. [2] introducing the idea of adapting a magnetic field sensor for biosensing in a giant magnetoresistance (GMR) prototype fabricated with well-controlled technology of a computer hard disc. The authors developed a method of detection of superparamagnetic labels and simultaneous characterization of many individual molecular recognition events called “bead array counter concept”. Since then, many attempts have been made aiming to develop a magnetic field based sensor adapted for biosensing on the basis of different physical phenomena [6-8].



- [6] M. Brzeska, M. Panhorst, P. B. Kamp, J. Schotter, G. Reiss, A Pühler, A Becker and H. Brückl, Detection and manipulation of biomolecules by magnetic carriers. *Journal of Biotechnology*, 112, (2004) 25–33.
- [7] G. V. Kurlyandskaya and V. I. Levit, Magnetic Dynabeads detection by sensitive element based on giant magnetoimpedance. *Biosensors and Bioelectronics*, 20 (2005) 1611-1616.
- [8] G. V. Kurlyandskaya, D. de Cos and S. O. Volchkov, Magnetosensitive Transducers for Nondestructive Testing Operating on the Basis of the Giant Magnetoimpedance Effect: A Review. *Russian Journal of Nondestructive Testing*, 45 (2009) 377-398.

THE BEAD ARRAY COUNTER CONCEPT



The detection principle for a GMR biosensor is detecting stray fields of magnetic markers “attached” to biomolecules of interest via appropriate biochemistry and translating them into an electronic signal [2]. First, the magnetic field detector is calibrated in the uniform external magnetic field. If superparamagnetic labels are present in the test solution, the application of the external field results in the appearance of magnetic moments of the spherical labels which can be calculated as stray fields of the magnetized spheres. As a result, for the same value of the external field, the effective field affecting the resistance value differ from the Hext value in the absence of the superparamagnetic labels. This difference can be quantified in terms of concentration if the number of magnetic labels is equal to the number of biomolecules of interest.

CLASSIFICATION OF MAGNETIC BIOSENSOR TYPES

Detection methods employing markers

Determining magnetic permeability by inductance measurements in Maxwell bridge (Kriz et al, 1996)

Measurements of the remanence of single domain magnetic nanoparticles bound to surface immobilized biomolecules (Matz et al, 1998)

GMR: Bead Array Counter (Baselt et al, 1998)

AMR: detection of single magnetic microsphere (Miller et al, 2002)

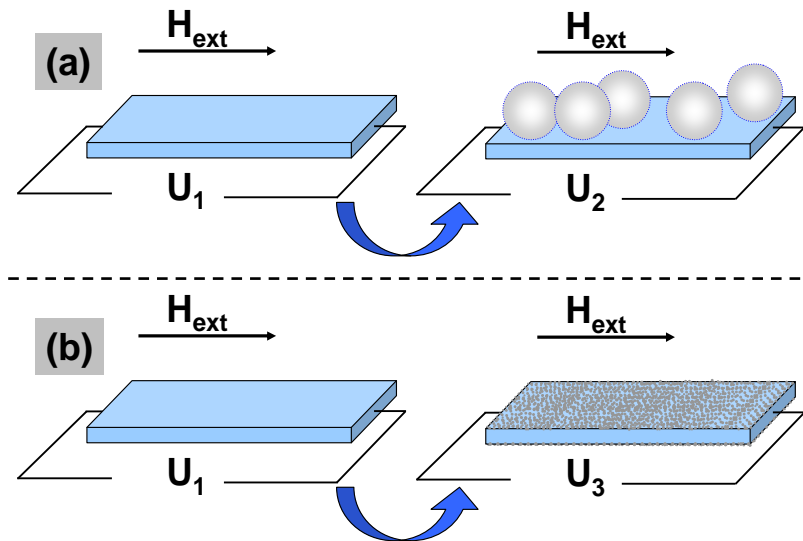
Spin-valves: integrated on-chip manipulation and detection of markers by magnetic gradient fields (Ferreira et al, 2002)

Hall effect for detection of single magnetic microsphere (Besse et al, 2002)

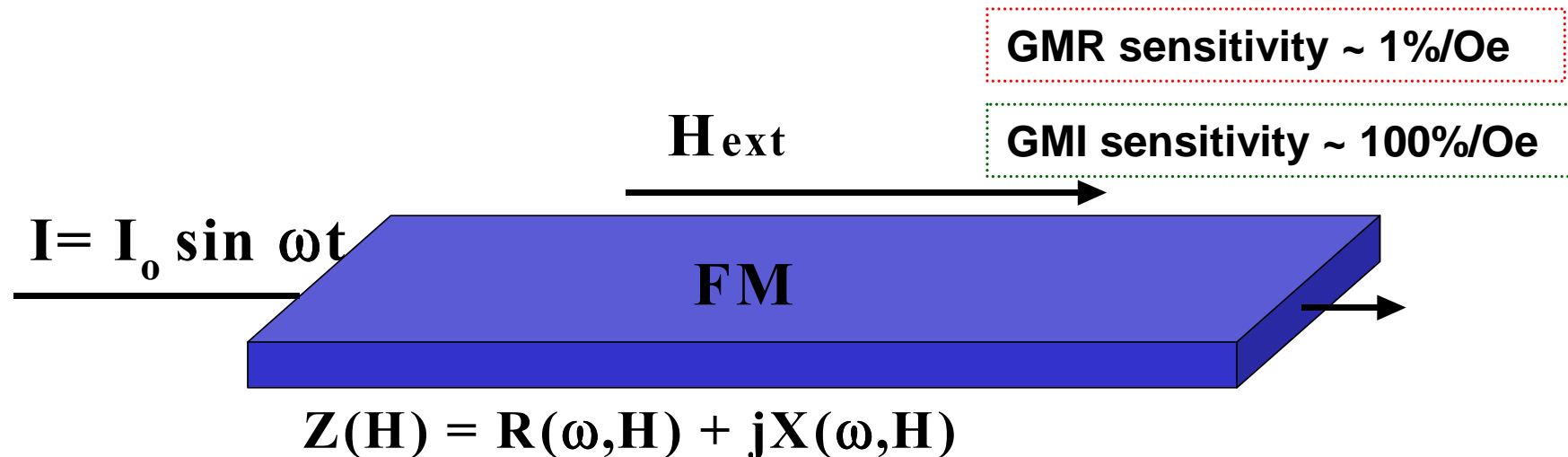
GMI: model experiment with ferrofluid (Kurlyandskaya et al, 2003) or microspheres (Bethke et al, 2003)

Detection of paramagnetic carbon nanotubes (A. Chaturvedi, et al, 2012).

Label free detection methods



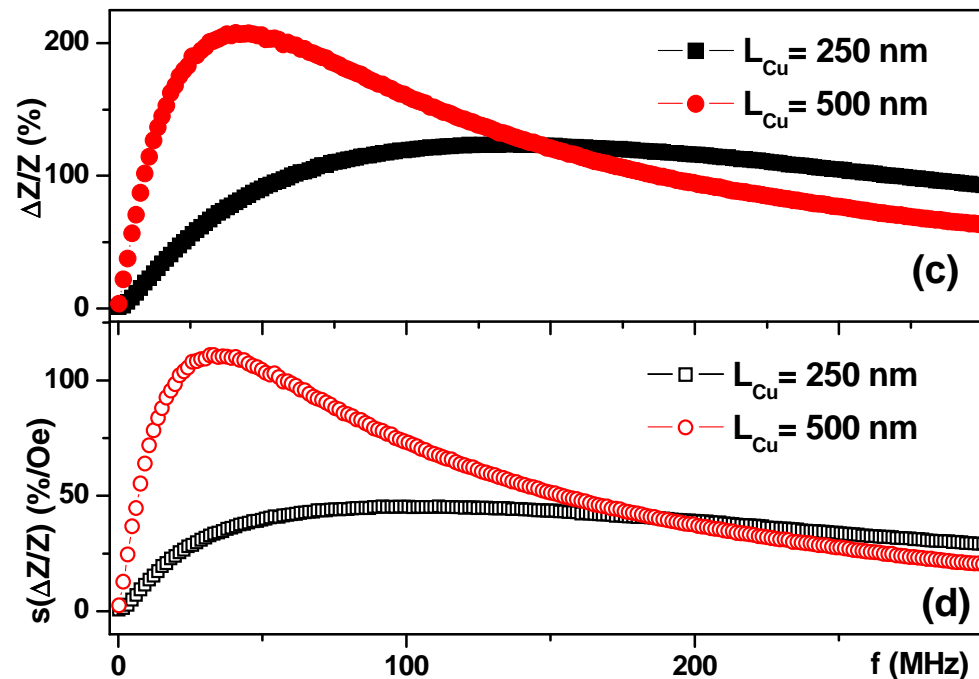
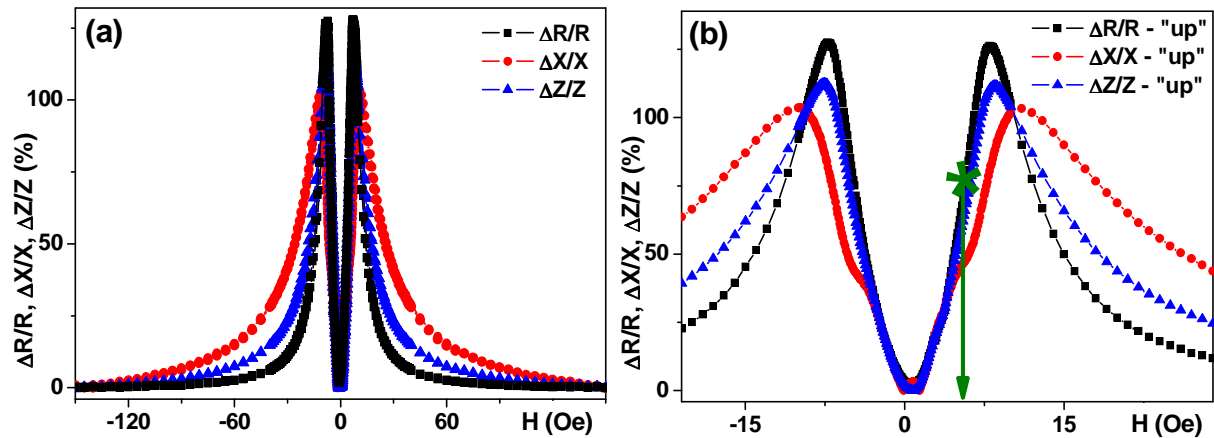
Two of the most important characteristics of the magnetic field detector are the sensitivity with respect to external magnetic field and magnetic field resolution [7-9]. Here we would like to give just one example related to GMR and giant magnetoimpedance effect (GMI). The **magnetoimpedance** phenomenon consists in the change of the total impedance of a ferromagnetic conductor, Z , under application of an external magnetic field when a high frequency alternating current, $I = I_0 e^{2\pi i f t}$, flows through it. $Z(f) = R(f) + iX(f)$, where R and X are the real and imaginary parts of the impedance, respectively and f is a frequency of the sinusoidal alternating current [9-10]; $|Z|^2 = |R|^2 + |X|^2$.



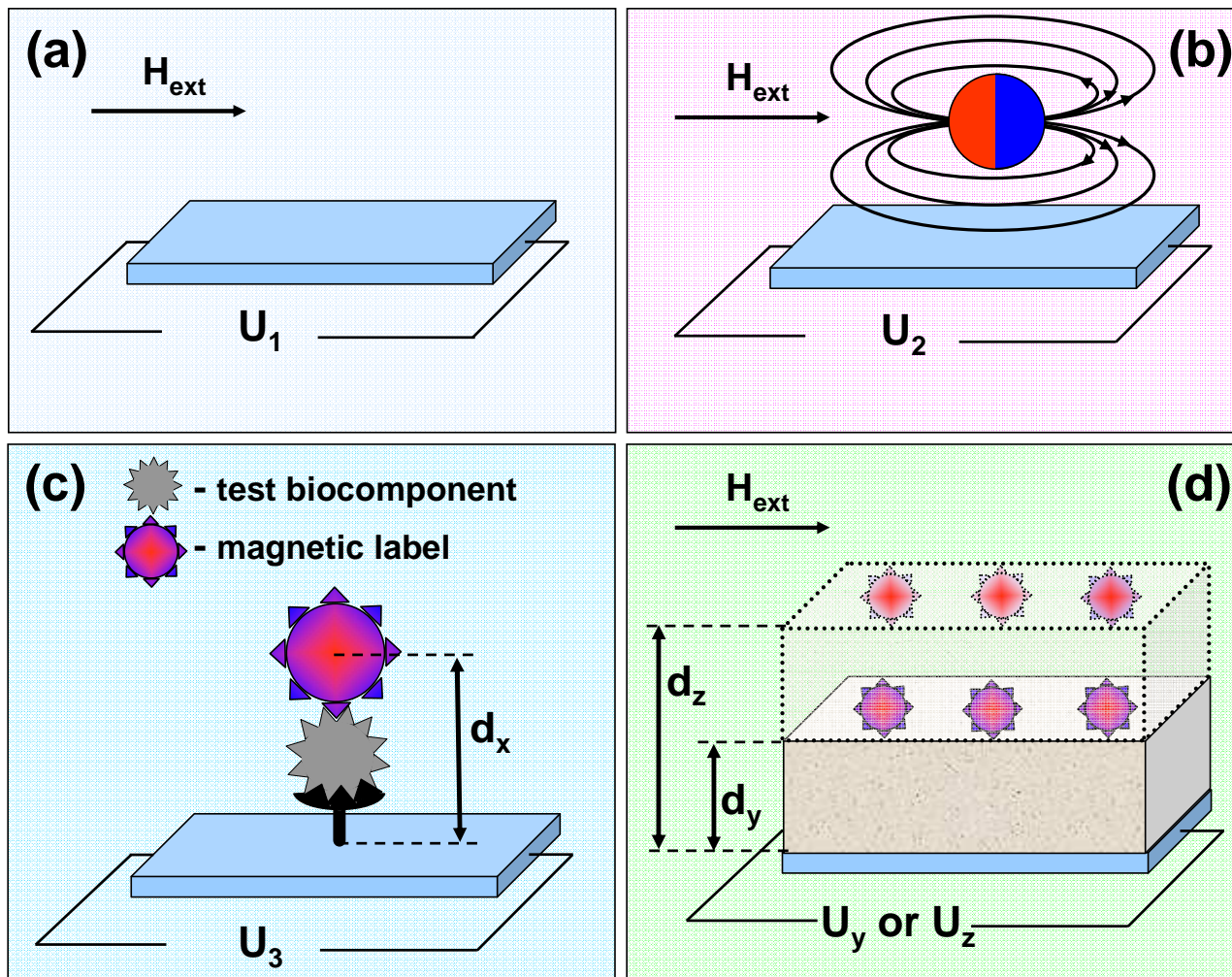
[9] V. E. Makhotkin, B. P. Shurukhin, V. A. Lopatin, P. Y. Marchukov and Y. K. Levin, Magnetic field sensors based on amorphous ribbons. *Sensors and Actuators A*, **759** (1991) 759-762.

[10] R. S. Beach and A. E. Berkowitz, Giant magnetic field dependent impedance of amorphous FeCoSiB wire. *Applied Physics Letters*, **64** (1994) 3652-3654.

[11] K. Mohri, T. Uchiyama, L. P. Shen, C. M. Cai and L.V. Panina, Sensitive micro-magnetic sensor family utilizing magneto-impedance (MI) and stress-impedance (SI) effects for intelligent measurements and controls. *Sensors and Actuators A* **91** (2001) 85-90.

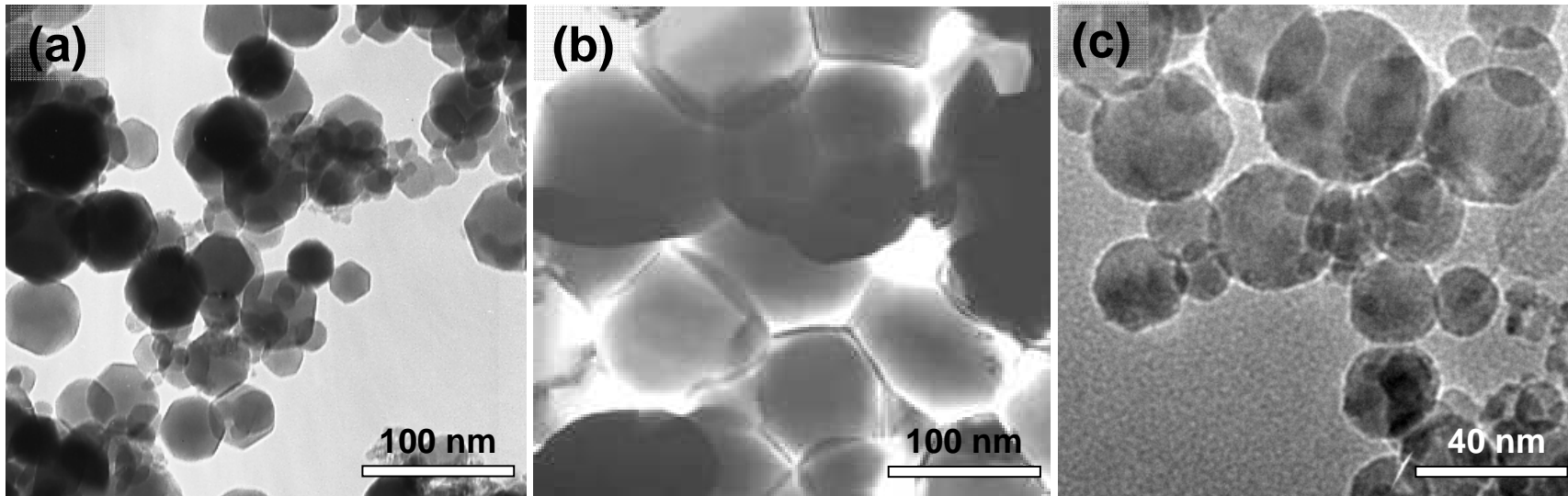


Field dependence of the MI ratios (“up” and “down” branches) for $[\text{FeNi}(170 \text{ nm})/\text{Ti}(6 \text{ nm})]_3/\text{Cu}$ (250 nm)/ $[\text{Ti}(6 \text{ nm})/\text{FeNi}(170 \text{ nm})]_3$ multilayers deposited onto Ciclo Olefin Copolymer flexible substrate at a frequency of 175 MHz (a). The same responses as in (a) shown for small field range: the highest sensitivity of about 30%/Oe (asterisk) corresponds to the real part (b). Frequency dependence of the maximum values of MI ratios for $[\text{FeNi}(170 \text{ nm})/\text{Ti}(6 \text{ nm})]_3/\text{Cu}(L_{Cu})/[\text{Ti}(6 \text{ nm})/\text{FeNi}(170)]_3$ multilayers deposited onto glass substrates (c). The highest sensitivity of about 110%/Oe corresponds to the frequency of 30 MHz for central Cu lead of $L_c = 500$ nm (d).



Description of magnetic biosensor functionality principle in the case of the external magnetic field applied in plane of the element. Initial calibration of the sensitive element for field interval under consideration: U_1 – is a voltage drop created at the ends of the sensitive element to calculate resistance for each field value in absence of magnetic labels in test solution (a). If superparamagnetic microsphere is present the stray fields are created under application of the external field affecting the resistance value: U_2 – is a voltage drop to calculate resistance in presence of magnetic labels in test solution (b). In the absence of an external magnetic field superparamagnetic label has zero net magnetic moment and U_3 – is a voltage drop at the ends. If all biochemistry was applied, a magnetic label with functionalized surface will appear at certain distance d_x from the surface of the magnetic sensitive element (c).

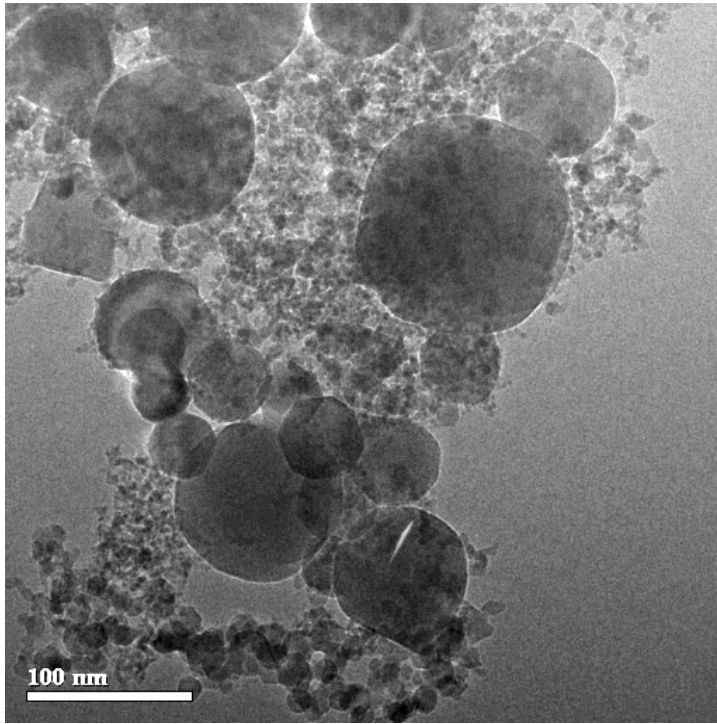
Magnetic labels are initially positioned on a surface of functional polymer at d_y distance from the surface of the magnetic sensitive element. After specific treatment (like water adhesion by hydrogel) the average distance is increased up to d_z . This change in distance is reflected in the change of average stray field value affecting the output signal of the sensitive element: the voltage drop at the ends of the sensitive element changes from U_y to U_z (d).



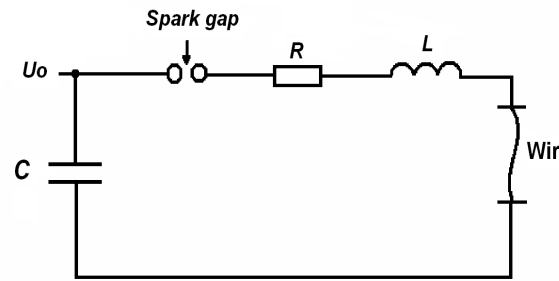
Magnetic nanoparticles can be synthesized by many different techniques including natural biomineralization [12-14]. Although visible progress has been made in fabricating spherical nanoparticles, the shape is still one of the most difficult parameters to control. In addition, modern drug delivery technologies demand a rather large amount of uniform material, a goal difficult to achieve using traditional chemical techniques. One of the relatively new techniques for spherical nanoparticles fabrication is - the method of electric explosion of wire (EEW) [16-17]. It is an efficient, ecologically safe and highly productive method based on the thermal dispersion of material in gas, providing production rates up to 200 g/h, for a small energy consumption of about 25 kWh/kg. EEW ensures a fabrication of both magnetic and non-magnetic nanoparticles with an average particle size of 20-100 nm and a high degree of sphericity.

[12] P. Tartaj, M. P. Morales, S. Veintemillas-Verdaguer., T. Gonzales-Carreño, and C. J. Serna, Synthesis, properties and biomedical applications of magnetic nanoparticles. In *Handbook of Magnetic Materials*, ed. K. H. J. Bushow (Amsterdam, Elsevier, 2006) 16, 403-482.

[13] Y.-W. Jun, J.-W. Seo and J. Cheon, Nanoscaling laws of magnetic nanoparticles and their applications in biomedical sciences. *Accounts of Chemical Research*, **41** (2008) 179-189.



Electric Explosion of wire (EEW)



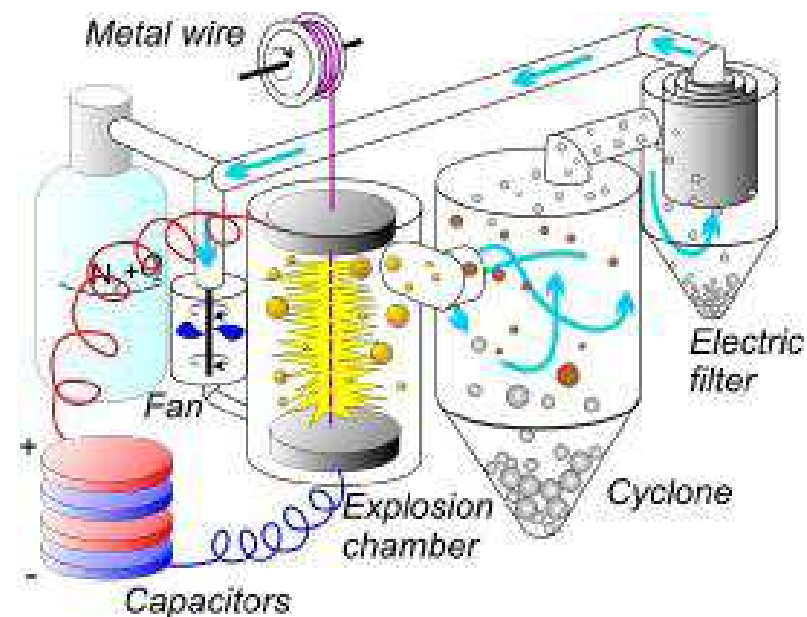
- $U_0 = 17 - 45 \text{ kV}$
- $C = 0.4 - 6.4 \mu\text{F}$
- Current pulse: 1- 3 μs , 20-100 kA

Yu. A. Kotov, Electric explosion of wires as a method for preparation of nanopowders. *Journal Nanoparticle Research*, **5** (2003) 539-550.





Electric Explosion of wire (EEW)

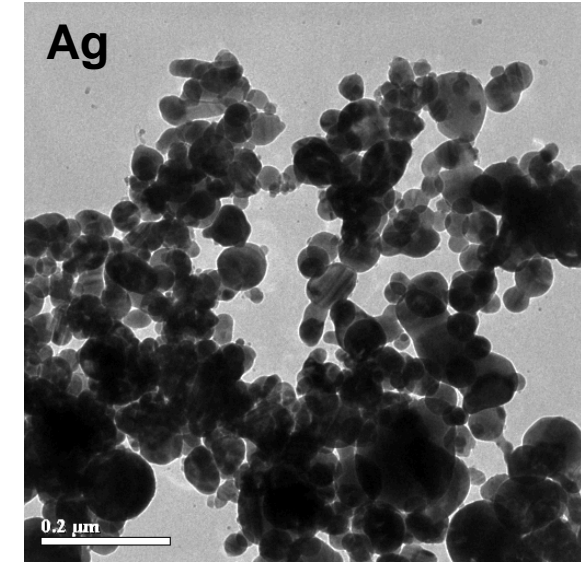
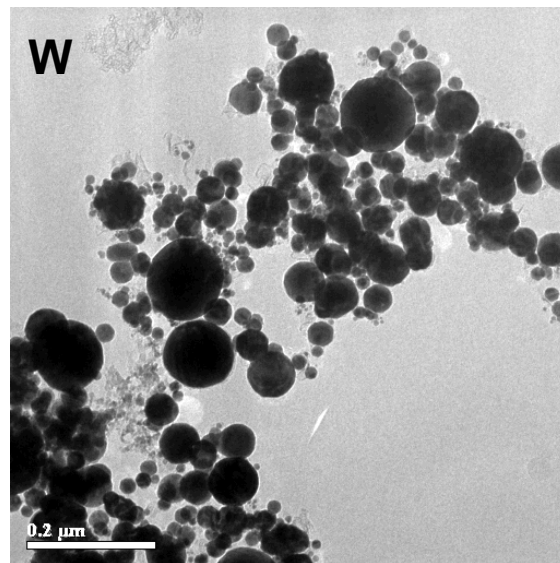
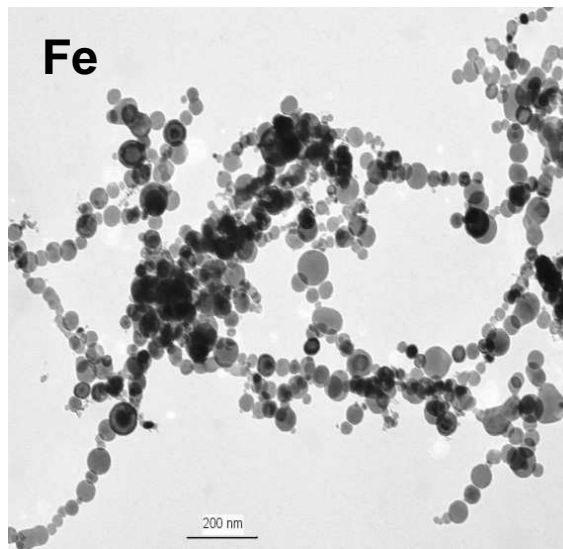
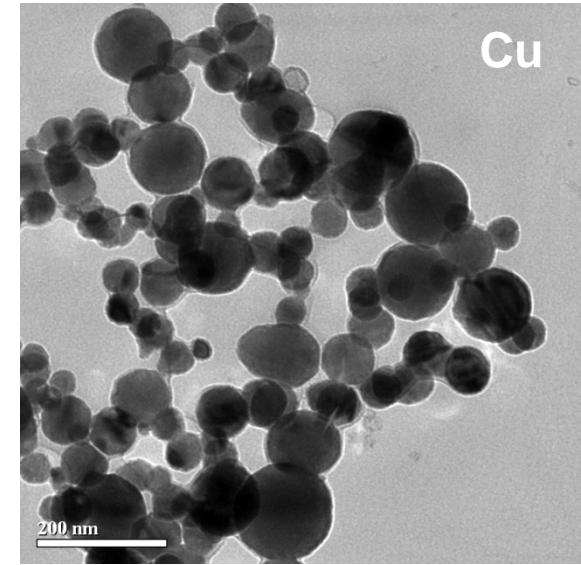
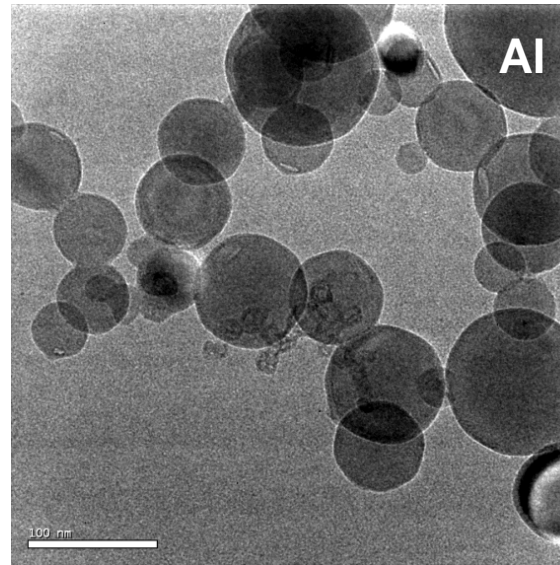
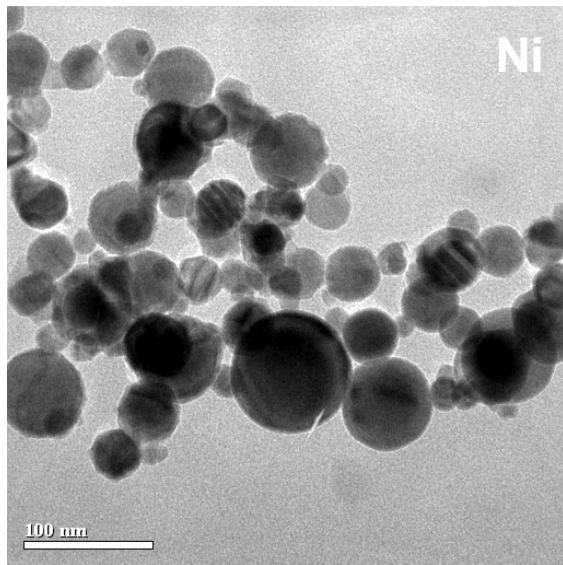


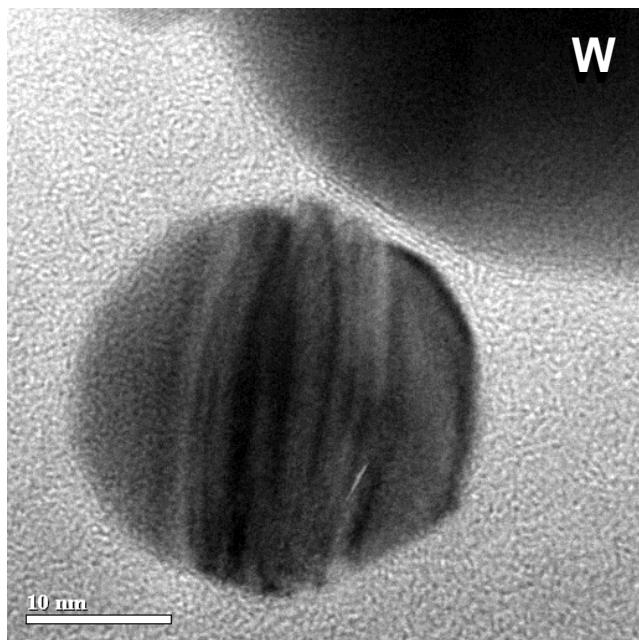
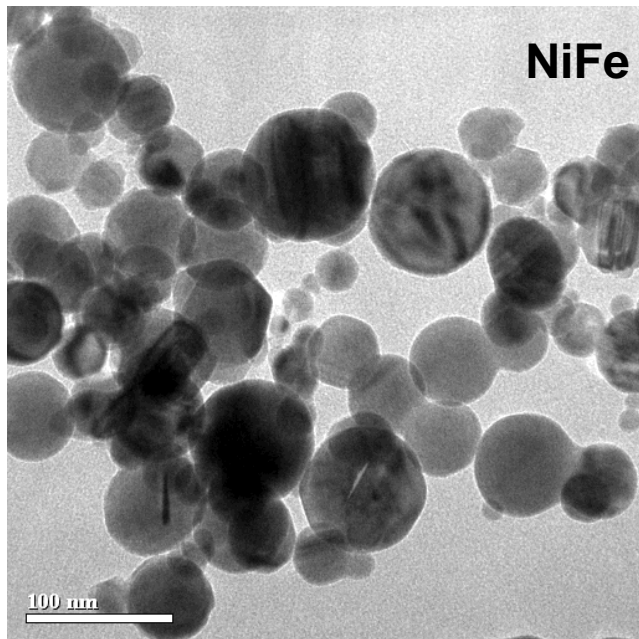
Amundsen str., 106, Ekaterinburg, Russia, 620016,
 Phone: +7 (343) 267-88-19, Fax: +7 (343) 267-87-94
www.iep.uran.ru

Wire:
 Dia. 0.2 - 0.8 mm
 Length 50 – 230 mm
 Working gas: Ar, N₂, He etc., gas mixtures
 Explosion frequency: up to 1 Hz
 Continuous operation
 Productivity: 100 – 400 g/h
 (depends on material)

EEW: metals and alloys

Courtesy of the Head of the Laboratory of Pulsed Processes, Institute of Electrophysics UD RAS Dr. Igor Beketov





EEW: metals and alloys

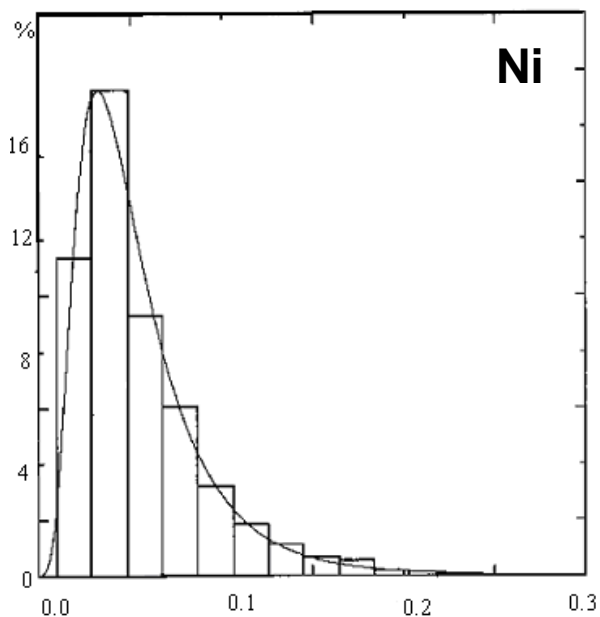
Nanopowders of metals: Al, Cu, Fe, Ni, Ti, W, Mo, Pt, Ag, Sn and others alloys: Cu-Ni, Al-Mg, Ni-Fe, Ni-Co and others.

With average particle size 50-100 nm.

Spherical shape

Low agglomeration

Particle size distribution: PSD = 1.7-2



The particle-size distribution (PSD) of a powder, or particles dispersed in fluid, is a mathematical function that defines the relative amount of particles present according to size. PSD is also known as grain size distribution.



EEW: compounds

Nanopowders of oxides and other compounds:

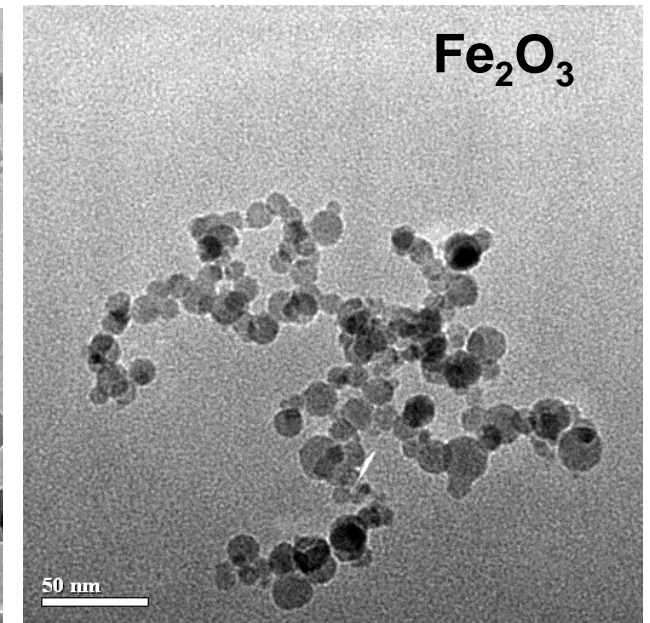
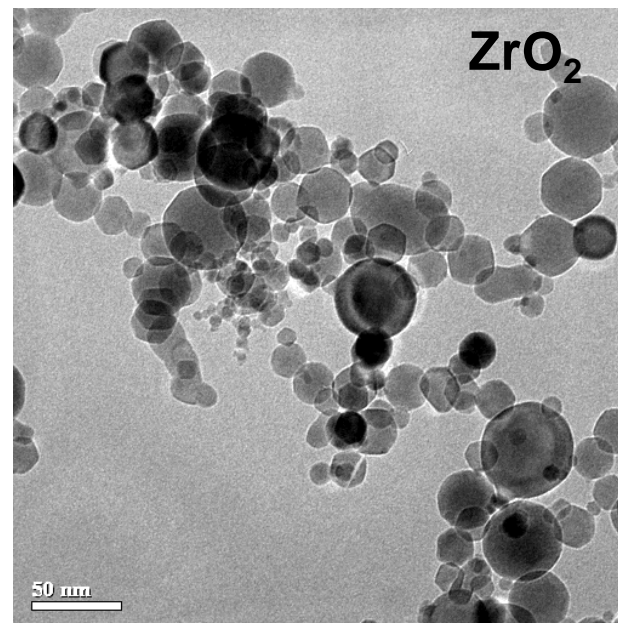
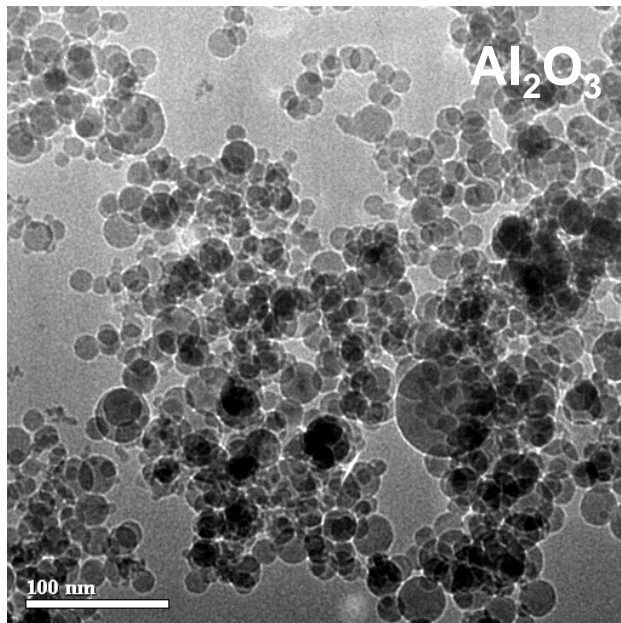
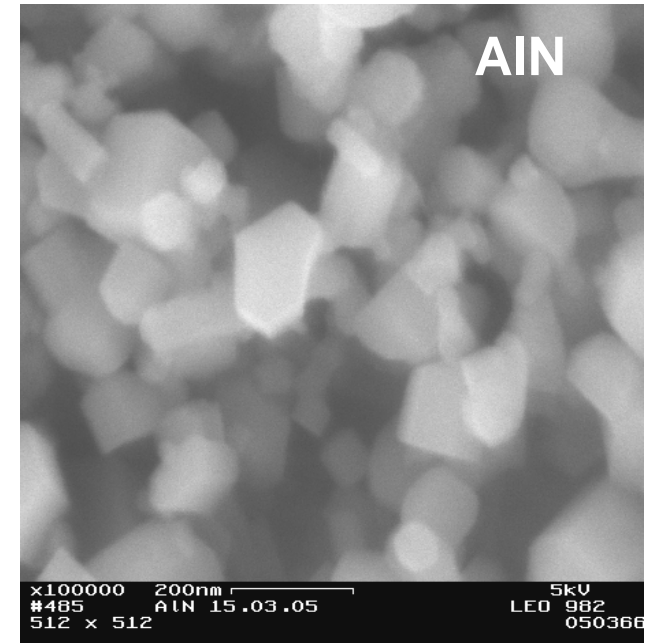
Al_2O_3 , CuO , NiO , ZrO_2 , Fe_2O_3 , ZnO , TiO_2 ,
 $(\text{MgAl})_2\text{O}_3$, AlN , TiN , Al_4C_3 and others with
average particle size 15-100 nm.

Spherical shape

Low aggregation

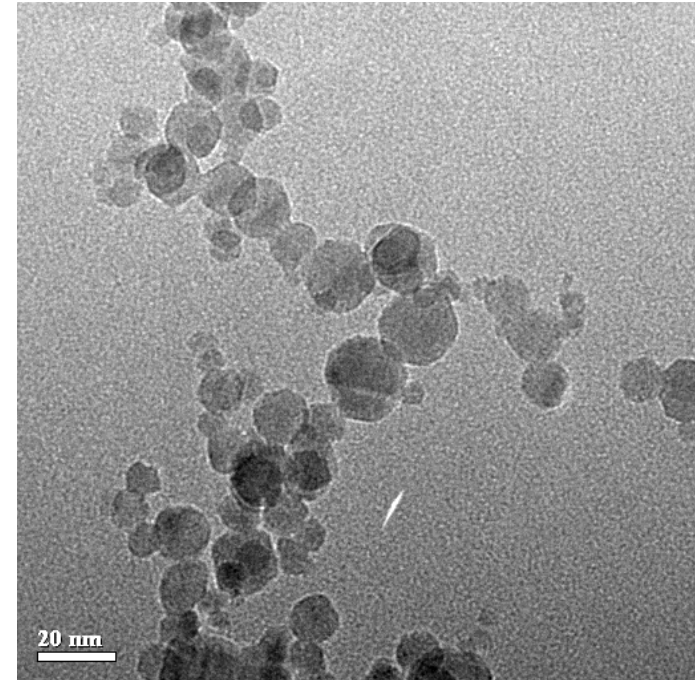
Particle size distribution: **GSD = 1.7-1.9**

A. P. Safronov, D. V. Leiman, D. N. Blagodetelev, Yu. A. Kotov, A. V. Bagazeev and A.M. Murzakaev, Aggregation of air-dry alumina powder nanoparticles redispersed in an aqueous medium. *Nanotechnologies in Russia*, 5 (2010) 777-785.



Ferrofluids are stable colloidal suspensions of ferro- or ferrimagnetic nanoparticles in a carrier chemically inert liquid. Good ferrofluids are stable with respect to gravitational forces and magnetic field gradients, and show no agglomeration under the effect of dipolar or Van der Waals interactions. The size of the particles is strictly limited by these conditions. Stability with respect to the field gradient is the most demanding factor leading to a general rule: the size of the nanoparticles of the ferrofluid should not exceed 10 nm. Two strategies were developed for the separation of nanoparticles: coating with a polymer layer (surfacted ferrofluids) and electrical charging of the particles for repelling due to Coulomb interaction (ionic ferrofluids).

The composition of a typical surfacted ferrofluid is about 5% magnetic solids, 10% surfactant and 85% carrier, by volume. For biomedical and pharmaceutical applications, aqueous ferrofluids have been developed.



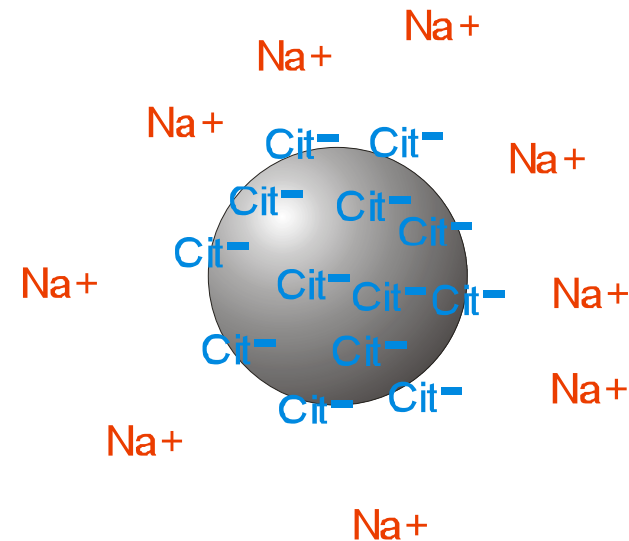
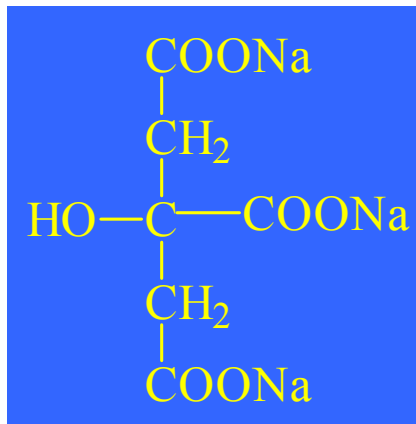
N. B. Adelman, K. J. Beckman, D. J. Campbell and A.B. Ellis, Preparation and properties of an aqueous ferrofluid. *Journal of Chemical Education*, **76** (1999) 943-948.

E. du Tremolet de Lacheisserie, D. Gignoux and M. Schlenker, *Magnetism. Materials and applications* (Boston: Springer, 2005).

G. V. Kurlyandskaya, M. L. Sanchez, B. Hernando, V. M. Prida, P. Gorria, and M. Tejedor, Giant-magnetoimpedance-based sensitive element as a model for biosensors, *Applied Physics Letters*, **82** (2003) 3053-3055.

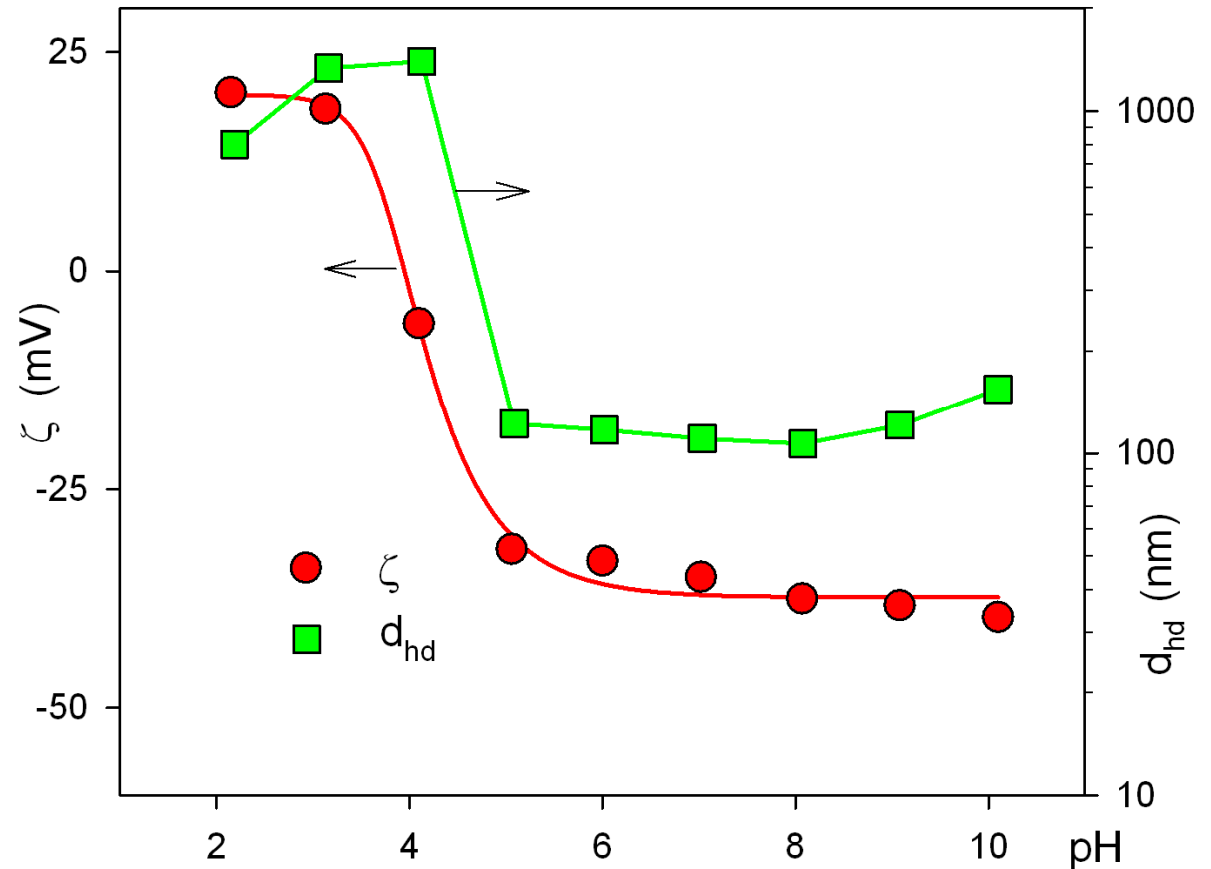
Electrostatic stabilization of magnetite suspensions by sodium citrate

One of the difficulties of practical applications of nanoparticles is connected with the fact that the air-dry assemblies of magnetic nanoparticles almost exclusively consist of aggregates formed by individual nanoparticles forced toward each other by strong magnetic interaction. Therefore, the necessary process of fractionation is very difficult but challenging. Beketov et al. (I.V. Beketov, A.P. Safronov, A.I. Medvedev, J. Alonso, G.V. Kurlyandskaya, S.M. Bhagat. AIP Advances. 2012. V.2. 022154) describe the preparation, fractionation and step-by-step characterization of ensembles of magnetic nanoparticles of iron oxide produced by EEW using different chemical and physical techniques. They succeeded to fabricate de-aggregated spherical magnetite nanoparticle ensembles with a narrow size distribution and the potential basis for the creation of on-purpose designed magnetic ferrofluids.



Electrostatic stabilization of magnetite suspensions by sodium citrate

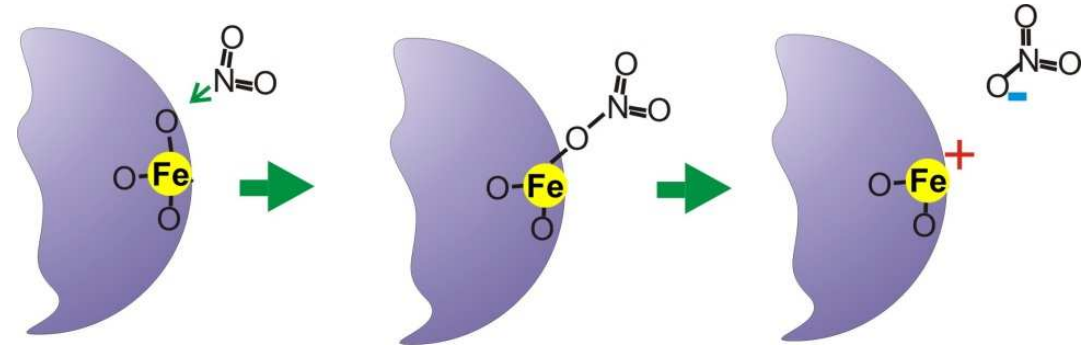
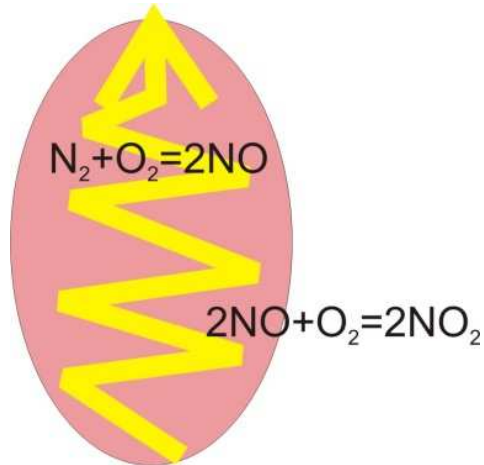
- Citric acid and its salts readily adsorb at oxide surfaces
- Adsorbed citrate anions provide negative electric charge on the particles
- The colloid stability of the suspension is achieved if zeta potential is larger than 30 mV irrespective of its sign
- Zeta potential of magnetite suspensions stabilized by citrate is below -30 mV if $\text{pH} > 6$. It makes suspensions stable in neutral and basic conditions



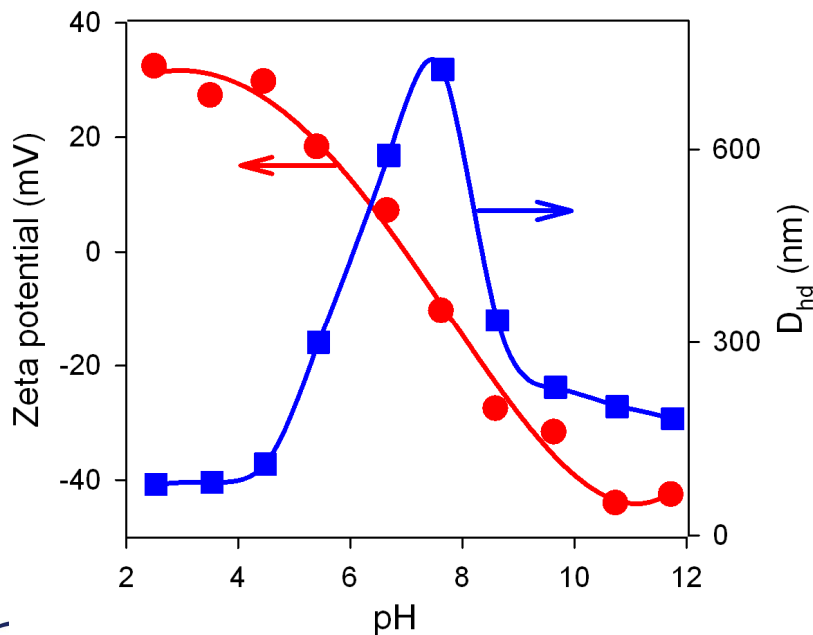
Courtesy of **Prof. Alexandr Safronov**, Department of Macromolecules, Ural federal University, Ekaterinburg, Russia.

Self-stabilization of EEW and LTE magnetite suspensions

During the electric discharge in the mixture of N_2 and O_2 traces of nitrogen oxides are synthesized by radical oxidation.



Nitrogen oxides react with the surface of oxide particles giving surface nitrates, which can dissociate in water. Nitrates are observed in mass-spectra of thermal analysis.

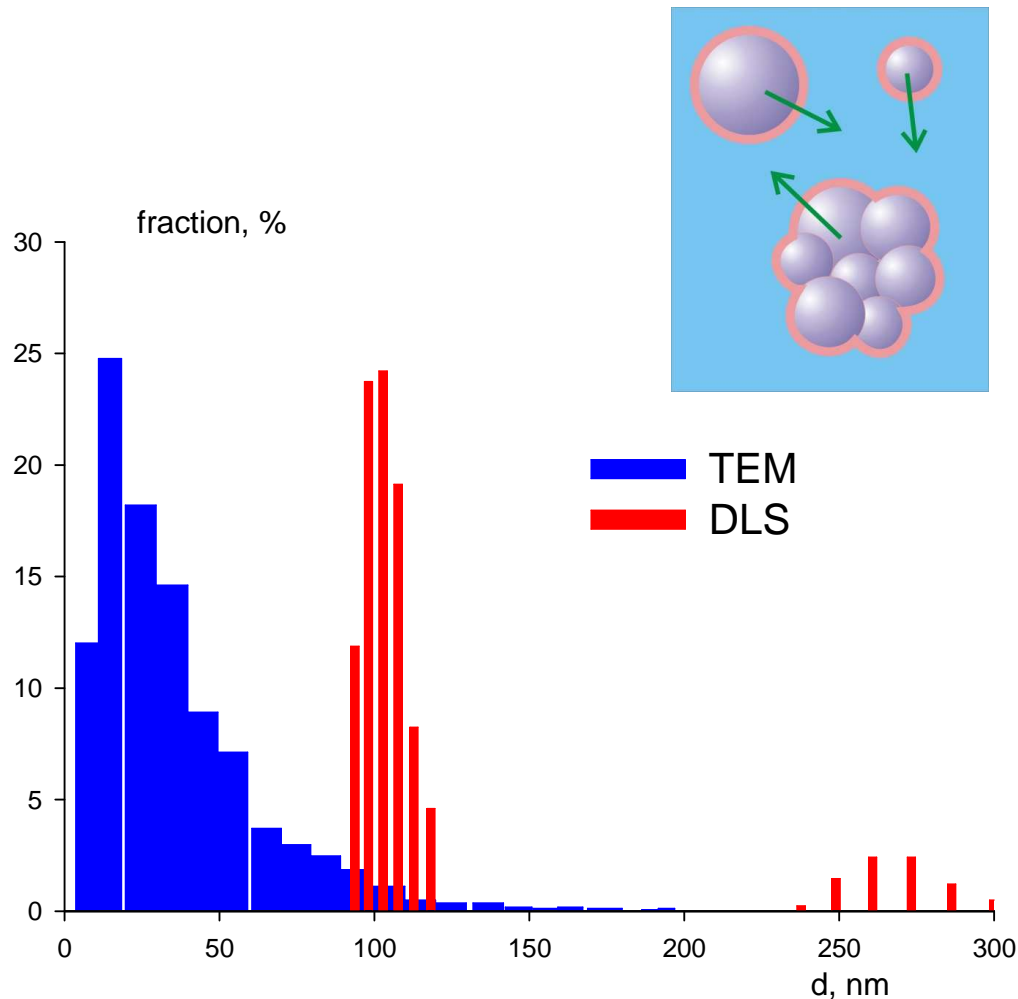


Dispersion of air-dry EEW NPs in water produce positive values of zeta-potential above +30 mV.

Self-stabilized suspensions are stable in acidic pH contrary to the suspensions with citrate.

A.P. Safronov, I.V. Beketov, S.V. Komogortsev, G.V. Kurlyandskaya, A.I. Medvedev, D. V. Leiman, A. Larrañaga, S.M. Bhagat AIP ADVANCES 3, 052135 (2013).

The average diameter in MNPs suspension is substantially higher than in air-dry sample!

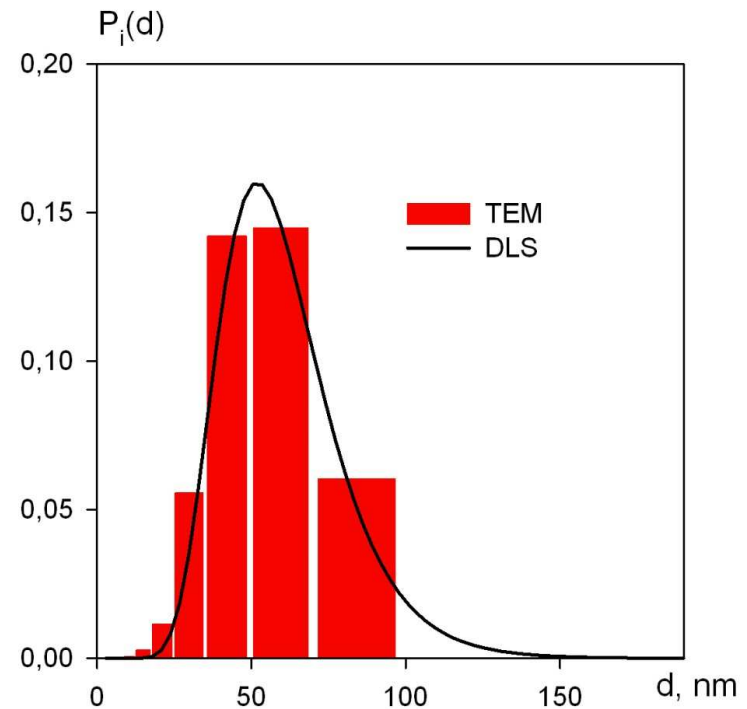
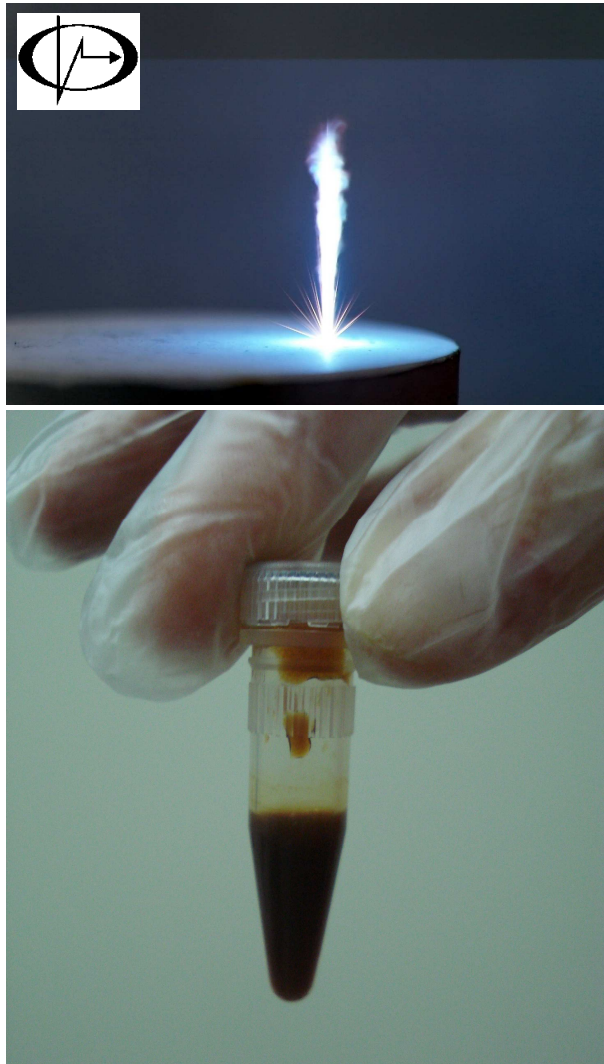


- The primary aggregates present in the air-dry sample preserve in suspension.
- The aggregates are small enough to be involved in Brownian motion.
- The primary aggregates are stabilized as quasi-particles, do not form secondary aggregates and do not precipitate.
- The major fraction according to DLS is around 100 nm, which is substantially higher than weight average diameter by TEM – 25 nm.
- Both the average diameter and the weight fraction of aggregates do not change upon the storage of the suspension.
- No precipitation is observed.

Intensity averaged PSD in de-aggregated suspensions of EEW and Laser Target Evaporation magnetite

- The evidence of de-aggregation is the correlation between PSD obtained by TEM and DLS.

As DLS is very sensitive to the presence of large particles and less sensitive to small particles better correlation is achieved in the intensity averaged PSD.



A. P. Safronov, I. V. Beketov, S. V. Komogortsev, G. V. Kurlyandskaya, A. I. Medvedev, D. V. Leiman, A. Larra.naga, S. M. Bhagat AIP ADVANCES 3, 052135 (2013).

EXAMPLES

The main goal of the study was to adopt the total reflection X-ray fluorescence (TXRF) analysis for measurements of iron concentrations in biological samples and to verify the obtained results by other techniques. Following parts can be outlined: a) adaptation of the method for prompt determination of iron concentration in yeasts samples containing absorbed nanomaghemite; b) optimization of sample preparation for measurements of iron concentration in ferrofluids in wide range of maghemite nanoparticles concentration.

Yeasts samples were successfully grown in nutrient medium with maghemite MNPs. Iron concentrations quantified by TXRF analysis were in good agreement with magnetic measurements. The method was shown to be suitable for prompt measurements required for prospective research.

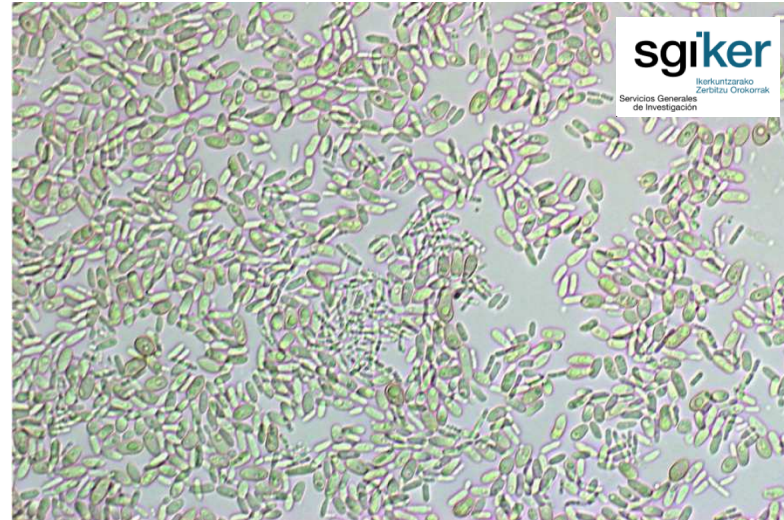


- Maghemite nanoparticles were obtained by LTE in purified $N_2 + O_2$ (0.79 : 0.21) flow;
- TEM photos were obtained by JEOL JEM2100 and PHILIPS EM208S electron microscopes;
- SEM photos were obtained by Hitachi S-4800 e and Hitachi S-3400 N electron microscopes;
- Number of cells was carried out by using LEICA LCS SP2 AOBIS optical microscope
- Geometry of dried drops was determined by contact profilometer Dectak-150;
- TXRF measurements were performed by using Nanohunter spectrometer (by Rigaku) with adjustable angle of incidence (0° to 2° with 0.01° step). For all experiments Cu X-ray tube was used.

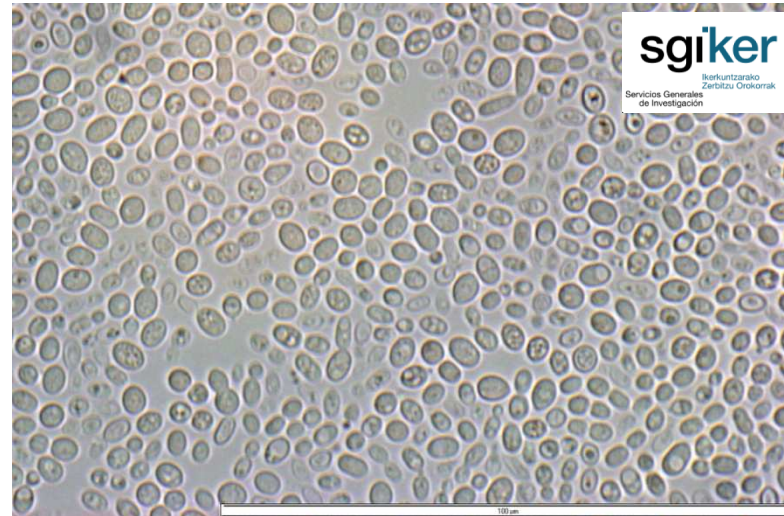
EXAMPLES

Yeasts samples characterization

Black yeasts

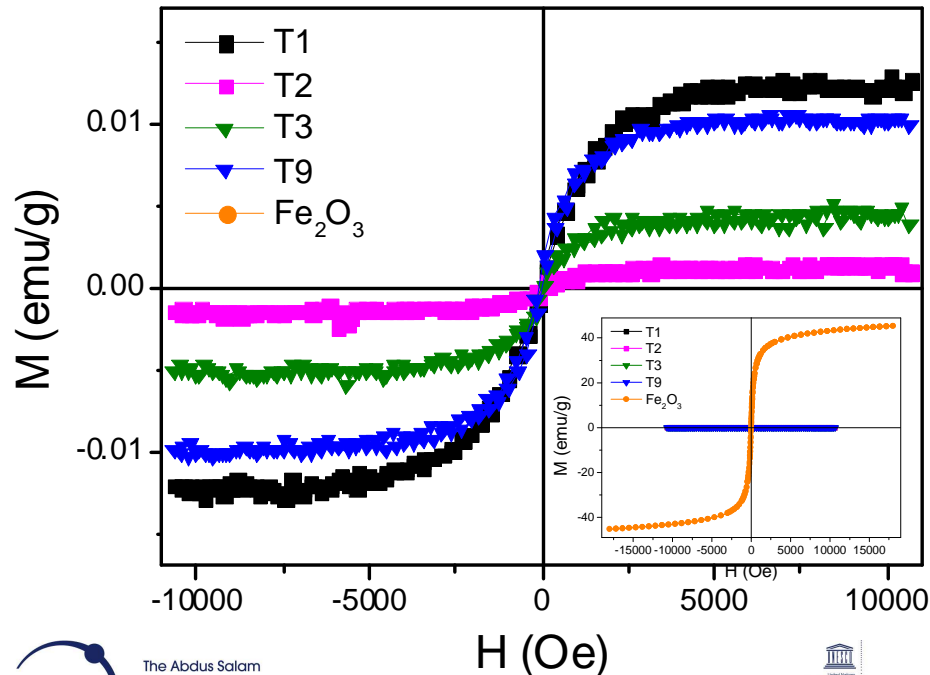
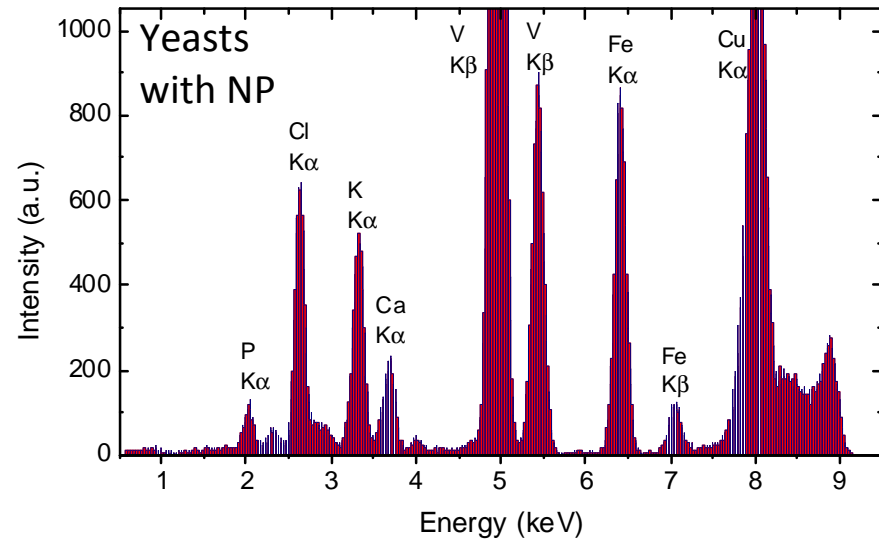
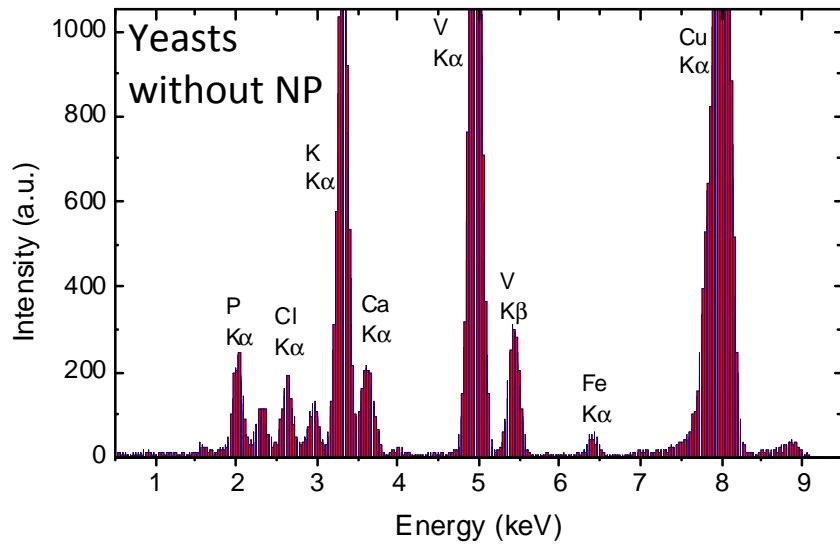


Red yeasts



EXAMPLES

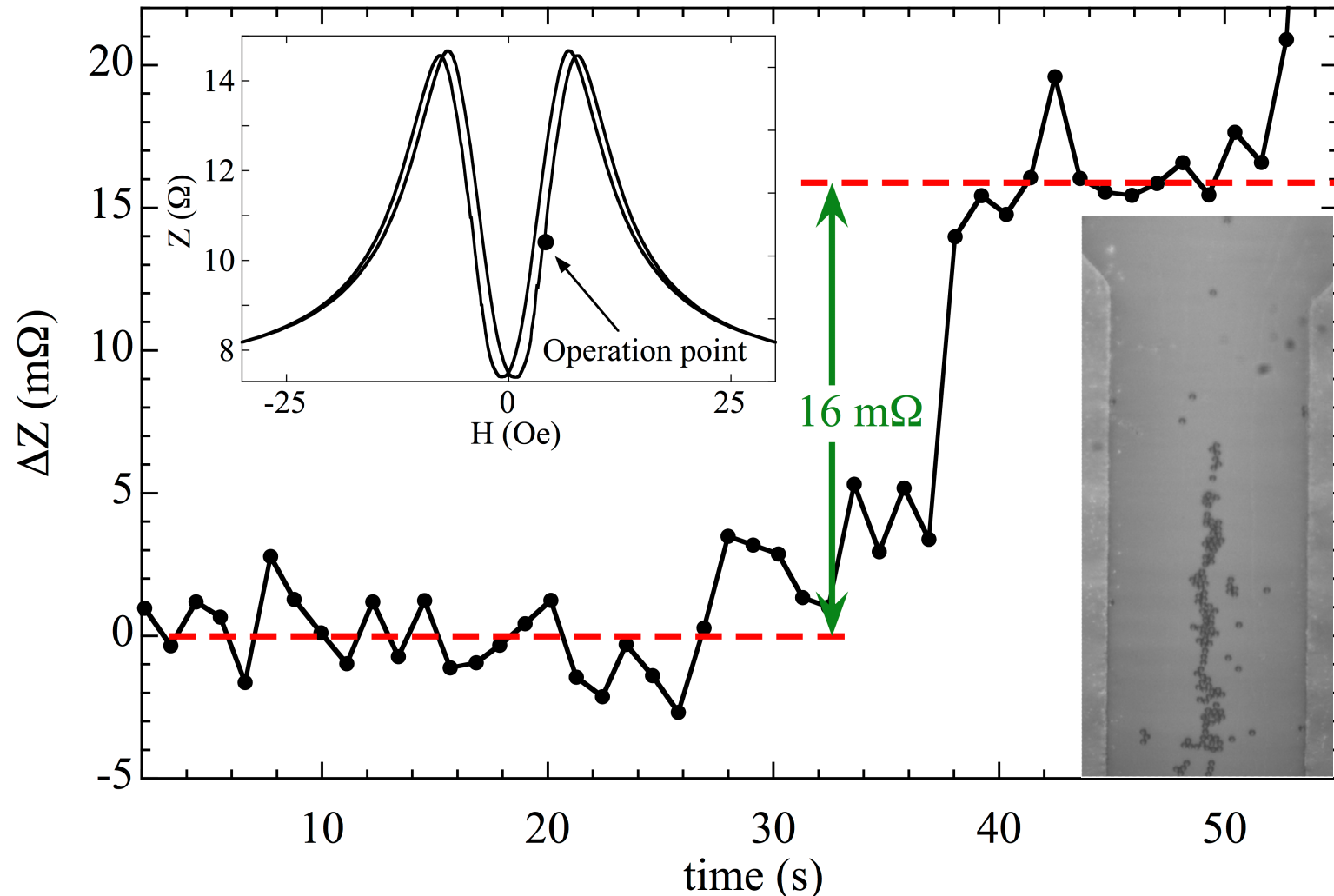
Exophiala nigrum (black yeast)



Sample	Type	M_s (emu/g)	C (pg/cell)
T1 Triton s	Red	0.002	0.1
T2 Triton n	Red	0.013	0.2
T3 Darvan s	Black	0.005	0.2
T9 Darvan n	Black	0.009	0.3
Fe_2O_3		45.3	

Courtesy **N.A Kulesh** and **J.P. Novoselova**, Ural Federal University

EXAMPLES

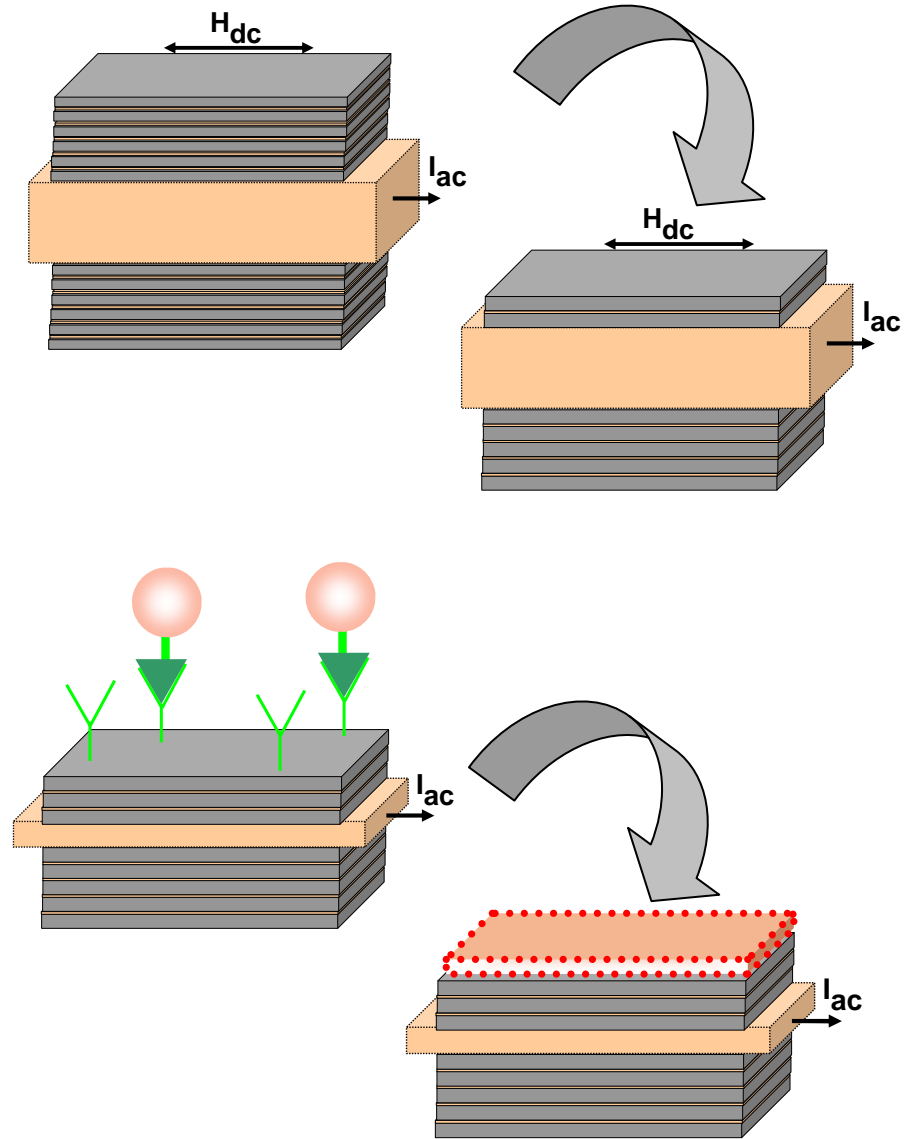
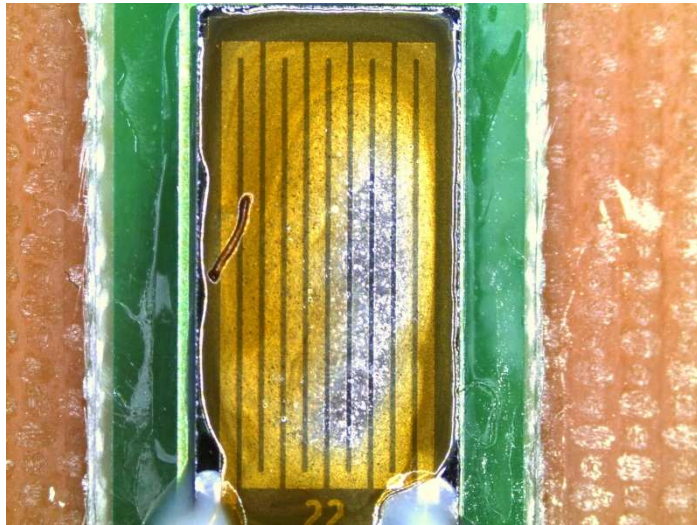
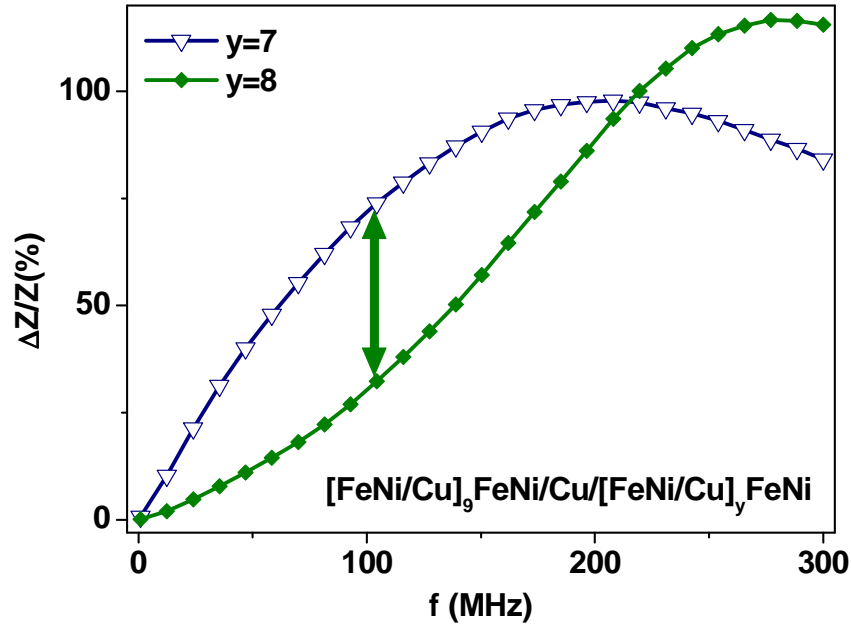


Impedance variation detected by $[\text{FeNi/Ti}]_3/\text{Cu}/[\text{FeNi/Ti}]_3$ element as a result of injection of Dynabeads M-450 in continuous flow. Inset: impedance of the FeNi-based multilayer as a function of the magnetic field, $f=180$ MHz; operation point $H=3.6$ Oe.

G. V. Kurlyandskaya, A. García-Arribas, E. Fernández, and A. V. Svalov, Nanostructured Magnetoimpedance Multilayers, IEEE TRANSACTIONS ON MAGNETICS, VOL. 48(4) 2012 1375-1380.

EXAMPLES

Non-symmetric MI structures as a solution for surface modified sensitive elements



IN COLLABORATION WITH

University of the Basque Country UPV-EHU, Bilbao, Spain: **A. Svalov, A. García-Arribas, E. Fernández, J. Alonso, M.L. Fdez-Gubieda, A. Larrañaga, R. Andrade**

Ural Federal University, Ekaterinburg, Russia: **A.P. Safronov, V.N. Lepalovskij, S.O. Volchkov, N.A. Kulesh, D.V. Leiman, A.A. Chlenova, J.P. Novoselova, V.O. Vas'kovskiy**

Institute of Electrophysics UD RAS, Ekaterinburg, Russia: **I.V. Beketov, N.I. Medvedev, O.M. Samatov, A.V. Bagazeev, A.M. Murzakayev**

University of Maryland, College Park, USA: **S.M. Bhagat**

East-Siberian State Academy of Education, Irkutsk, Russia: **T.P. Denisova, K.A. Zarubina**

Institute of Physics L.V. Kirensky 660036, Krasnoyarsk, Russia: **S.V. Komogortsev.**

This work was supported by project no. 215 “Magnetodynamics of High Permeability Nanostructured Media” at the Ural Federal University and SAIOTEK “REMASEN” grant of UPV-EHU. Selected measurements were performed at SGIKER of UPV-EHU.

